THE EFFECTS OF TURBULENCE STRUCTURES ON THE AIR-SIDE PERFORMANCE OF COMPACT TUBE-FIN HEAT EXCHANGERS

By

Colin Bidden Allison

A Thesis submitted in fulfilment of the requirements for the
Degree of Doctor of Philosophy

SCHOOL OF MECHANICAL ENGINEERING
UNIVERSITY OF ADELAIDE

June 2006

Chapter 1

Introduction

Heat exchangers have become an essential part of our modern commercial, industrial and technological age, and the range of heat exchanger types is as diverse as the number of different processes or applications available. Tube-fin heat exchangers comprise a specific category which includes a broad range of heat exchangers to suit particular applications. These include large scale industrial and chemical processes, air conditioners for comfort applications or compact micro heat exchangers used in the aeronautical or space industries. Generally, the applications of these heat exchangers involve either a temperature or phase change of a fluid, resulting in the absorption or rejection of energy in the form of heat. Because of their widespread applications, they are responsible for transferring enormous amounts of energy. Since global energy consumption is starting to impact negatively on the environment, as well as causing depletion of our existing fuel stocks, energy utilisation has come under close scrutiny. Since heat exchangers are an integral component of the dissemination of energy, their effectiveness is becoming crucial to our lifestyle sustainability. Clearly the motivating factor in pursuing the current study is a consideration of energy consumption and consequently the impact on Green House gasses. In air conditioning applications for example, tube and fin heat exchangers are used as cooling coils. As far back as 1994, The South Australian Office of Energy reported that 43% of the energy used in commercial buildings is consumed by air conditioning systems[1]. This is clearly an appreciable amount of energy that is ultimately transferred through both the evaporator coil as well as the outdoor condensing system. Thus, any improvement in either heat exchanger effectiveness, resulting in lower energy consumption, has worthwhile benefits.

Tube-fin heat exchangers are employed to facilitate heat transfer between a gas and a liquid. Generally, the liquid of which heat is to be exchanged, is pumped through a

system of compactly arranged tubes, while the gas having lower density and heat capacity thereby occupying a greater volume, is driven over the outer tube surfaces. In order to compensate for the lower heat transfer capacity of the air, fins are employed to increase the heat transfer area, hence the term "extended surface heat exchanger". Unfortunately, the fin density required to achieve practical heat transfer performance in a compact design, results in the air flow remaining laminar at all times. The laminar air-flow is associated with thick developing boundary layers, which impede heat transfer performance. This limitation and the desire to improve heat transfer performance with reduced material and manufacturing costs continue to motivate research in gas side heat transfer enhancement.

The operating temperatures of tube-fin heat exchangers can range from, minus 40 degrees Celsius in freezer room applications, to 95 degrees Celsius in radiator applications. In many applications condensation of the gas on the fin and tube surfaces takes place, which is an inevitable and in some cases desirable consequence of the heat and mass transfer process. In chilled water air conditioning systems where dehumidification takes place during the air-cooling process, the heat exchange is a two-phase flow on the airside resulting from water condensation on the heat exchange surface. The transfer of heat by a two-phase flow mechanism is higher than that for single phase flow as a consequence of latent heat exchange. However, there are applications where the heat transfer mechanism can be characterised by single-phase flow only, and it is desirable to maximise the transfer of sensible heat only. Some obvious examples are industrial radiators and condensing units, or chilled water air conditioning cooling coils serving a non-humid environment such as a computer room, or as is now very common in most developed countries, computer data centres[1].

Until fairly recently water cooled heat exchangers were used extensively to reject heat from buildings or industrial processes. Water-cooled heat exchangers are more efficient because they reject most of the heat via latent heat rejection. Assuming a reasonable maintenance programme, they are less prone to corrosion problems than air-cooled

[1] Commercial Data Centres typically have cooling heat loads of 900 Watts per square meter and extensive floor areas. An average sized Data Centre with a co-location area of 5000 square meters or more would therefore have extremely high cooling demands and consequently high energy requirements.

condensing units. However, due to recent outbreaks of Legionaires disease, resulting in several fatalities, the cause of which is normally traced to the local evaporative cooling towers, a solution is called for. Government Legislation and recently adopted standards calling for an equipment registration and regular maintenance regime have made the evaporative cooling tower more problematic than it is worth. Practitioners and designers are electing to forsake the efficiency of the evaporative condensing unit in favour of the more convenient air-cooled condensing unit. In comparison, air cooled condensers operate at higher temperatures and condensing pressures and therefore require more compressor work. This means that more energy is being transferred by less efficient means, and hence there is enormous potential for an alternative to the current range of air cooled condensing units.

Much of the pioneering work in heat exchanger design, was done by Kays and London[2] back in the 1940′s. This work has formed the basis for many designs ever since. Although, their work was comprehensive and covered many configurations of tube and fin designs, it was influenced by the manufacturing techniques that were available at the time. The fundamental considerations that Kays and London addressed in the fourties are still current now. The performance of heat exchangers is measured by their ability to transfer a maximum amount of heat with the least pressure drop, while satisfying weight and spatial constraints. In addition to performance, economic considerations have had to be addressed. These days, the true cost of a cooling coil is measured in the material and running costs rather than in the manufacturing cost. This stems from the fact that manufacturing costs have been decreasing in the last two decades, with the introduction of automated systems and mass production of components. In comparison, the cost of raw products such as steel and copper, as well as energy costs has risen dramatically.

Some variations of the standard designs have been suggested in the last two decades, especially when energy supply shortages such as during the 70′s and more recently environmental concerns have been driving governmental policies. However, no serious examination of the current designs has been conducted in the last two decades. Many researchers have concentrated their efforts on trying to improve the airside heat transfer coefficient. Most of the techniques involve some sort of fin surface perturbation leading to the term “enhanced surface” heat exchanger. As expected,

most of these surface perturbations cause an increase in pressure loss. As a result there has been limited improvement in the overall performance. In fact in most cases the increase in penalty due to pressure loss has far exceeded the heat transfer performance improvement.

With respect to heat transfer potential, the main resistance is the airside heat transfer convection coefficient. In typical applications, of the tube-fin heat exchangers, the airside resistance comprises over 90% of the total thermal resistance[3]. It has been demonstrated through some simplified calculations[4] that the air side resistance is in the order of 150 times greater than that of the tube side resistance and 6000 times that of the conduction resistance. As it is the airside resistance which is the limiting factor, reducing the tube side resistance or the conduction resistance, can only result in a minimal overall improvement.

There are essentially two approaches to reducing the airside resistance. One approach is to increase the heat transfer surface area by increasing the fin density. The other approach is to improve the convection coefficient by promoting turbulence through fin surface enhancement. Increasing the fin density increases the coil capacity albeit according to the law of diminishing returns. This is because reducing the fin spacing results in excessive laminarisation of the flow, and any turbulent or vortical motion is quickly dissipated by both mechanical blockage and skin friction from the increased surface area. Apart from increased manufacturing requirements and material costs, using more material imposes a weight penalty, which may restrict the range of applications available. In addition, there is an associated increase in pressure drop and an increase in fouling and blockage potential. Thus by increasing the fin density there is a trade-off between increased capacity versus pressure loss and cost, as well as reduced performance reliability. Consequently increasing fin density may increase the coil capacity but at the same time it reduces the coil effectiveness and hence increases energy wastage.

Enhancing the fin surface is achieved by modifying the fin surface geometry. There seems to be no limit to the intricacy or creativity of the various surface enhancements suggested. The variety of surface perturbations incorporated meet with varying degrees

of improvement, none of them remarkable. They all have a resulting higher pressure drop. In addition these methods are usually associated with an increase in either manufacturing costs, manufacturing complexity, or material costs. Successive generations of fin surface enhancement techniques have evolved, and each generation employs different heat transfer mechanisms[5]. Firstly there were the wavy and dimpled surfaces, which relied on changing the direction of the flow to impose velocity gradients and hence cause localised increase in temperature gradients. The next generation comprised the slit and louvred surfaces, which facilitated boundary layer renewal. The third generation employ longitudinal vortex generators in the shape of rectangular or delta winglets. The imposed vorticity supposedly provide enhanced heat transfer performance with relatively low penalties in pressure loss. This type of vortex generator is currently stimulating much interest and ongoing research. However, their benefit in a compact tube-fin heat exchanger is yet to be conclusively demonstrated.

A central consideration in the optimisation of a heat exchanger is the particular application or operating conditions it is likely to encounter. Indoor air conditioning coils should be compact and light to comply with spatial requirements. They are normally protected by air filters, and therefore not likely to encounter fouling problems. Automobile radiators should also be compact and light but are more likely to become fouled in the absence of any filter protection. Industrial radiators or outdoor condensing units are not subject to the same space or weight constraints but are prone to performance degradation due to fouling and corrosion especially in industrial or harsh environments. Freezer room evaporator coils may experience frosting up of the fins and therefore they usually are designed with wide fin spacing. Typical air velocities encountered by cooling coils range from 1.5 to 2.5 m/s while for radiators the range is from about 4.0m/s to over 7.0 m/s. Considering this diverse range of operating conditions and varying performance requirements, it is unlikely that a generalised enhancement could be applied across the assortment. Clearly the heat exchanger application and intended operating conditions require to be taken into consideration. The specific area of interest studied in this work involves the enhancement of the performance of commercial louvre fin radiator coils having flat tubes in a staggered arrangement hence only sensible heat exchange performance is considered.

It is thought that enhancement may be achieved by modifying the flow character occurring in fin type heat exchangers. It is well accepted, though maybe not well understood, that increased turbulence and vorticity enhance heat transfer. However, there are several different categories of turbulence. For example homogeneous turbulence as generated by a grid mesh has a flow character that is by definition three dimensional and is therefore not normally associated with the typical laminar flow occurring in fin type heat exchangers. Kays and London[2] have measured the pressure drop of various types of grid meshes, but the heat transfer performance of a tube mesh has not been undertaken. A liquid-air heat exchanger comprising solely of tubes arranged in a turbulence generating mesh would supplement our existing knowledge base of heat transfer resulting from an approximation of homogeneous turbulence.

Vortex generation may usually imply the presence of a turbulent flow. Numerous turbulent or laminar vortices have been categorised, and many of these are identifiable in the flow characteristics occurring in various heat exchangers. Some of these are active in nature, while some are passive. Active methods require external power such as electric or acoustic fields, mechanical devices or surface vibration. Passive methods do not require any external power but make use of special surface geometry or fluid additive. Enhancements that simultaneously use more than one method are referred to as compound methods[6]. There has been very little work directed at active vortex methods in a heat exchanger application. This disinclination is probably due to increased capital and operating costs, as well as potential operating problems.

It seems that there is far more practical potential in creating vortices using passive methods, and there is one method that has particular merit. It is not well known that a series of flat plates arranged in a staggered array can induce transverse vortices in a passive manner. There have been several studies undertaken to investigate the characteristics of transverse vortex shedding in plate arrays. Dejong and Jacobi[7] were able to measure local and average heat transfer coefficients using a mass transfer analogy. They found that in comparison to a continuous plate, there was up to a 40% increase in overall heat transfer coefficient due to vortex shedding. There was also another 40% increase over the continuous fin result due to boundary layer restarting.

Thus there seems to be tremendous potential for heat transfer enhancement if this technique could be incorporated into a tube fin heat exchanger design.

The delta-winglet vortex generators spoken of earlier generate longitudinal or more specifically streamwise vortices. These are thought to enhance convection coefficients to a greater degree than transverse vortices. Streamwise vortices are generated as a result of introduction or exploitation of secondary flows rather than a manipulation of the bulk fluid flow. Therefore improved heat transfer can result with minimal pressure drop penalty. Several studies have been undertaken to assess the potential of this type of vortex generator to enhance heat transfer[8-10]. Various delta orientations and positioning relative to the tube have been studied. There is no evidence to show that they are used in a commercial application, and it can be assumed that the reason for this is that no satisfactory configuration has been found to achieve acceptable performance improvement. Therefore there is scope for examining the potential of alternative delta-winglet configurations and a previously untried configuration is examined in this study.

There has been some interest in the likelihood of improving the performance of a louvre surface by including vortex generators in combination with the louvres. However, it appears that mixed results have been achieved by various researchers[11, 12]. An increase in heat transfer of 21% has been reported on one hand, and actually a decrease on the other. Hence there is scope for further investigation into the merits of combining vortex generators with louvre surfaces.

The optimisation of the standard louvre fin surface has been investigated and is normally proprietary privileged information. Variation in the louvre angle and pitch are numerically assessed. Interestingly, something that has not been previously considered is the possibility of optimising the standard louvre surface by serrating the louvre edges, in lieu of having straight edges. It is thought that this may effectively increase the leading edge length, and the serrations may generate micro vortices to wash the louvre surfaces. Up until now such a modification would be difficult to implement on a small scale. However with the current CFD tools available it is thought fitting to investigate the potential of this type of modification without any manufacturing investment.

Several turbulence mechanisms have been identified and this behoves the investigation of these in the context of heat exchanger applications. The objective is to perform a series of experiments in order to accumulate further understanding of the enhancement of heat transfer as a result of turbulence and secondary flow structures occurring in heat exchangers. Experiments have been conducted to distinguish the various types of turbulence within the framework of practical heat exchanger applications. This is achieved by the fabrication and testing of novel heat exchanger prototypes. The results are complimented with flow visualisation techniques and numerical simulations.

The following chapter consists of a comprehensive literature review. It was essential to cover a broad range of categories since inspiration comes from a conglomeration of ideas and knowledge. It was considered especially pertinent to examine the potential of unconventional or novel heat exchanger designs. The findings have been structured in the form of a database, which attempts to categorise various design aspects and their corresponding contributions to heat transfer and pressure drop.

This is followed in Chapter 3 by a general yet detailed report of the experimental techniques, equipment and methodology. The proposed heat exchanger prototypes have been experimentally assessed on a purpose built heat and mass transfer rig. In general all of the proposed prototypes and standard coils have been assessed using precisely the same test conditions. Where specific test conditions may be required, these are outlined in the relevant chapter. The flow visualisation equipment and techniques are also described.

Chapter 4 contains a fundamental outline and theory of the relevant Numerical Techniques used and the commercial CFD code description. The computational models which were used to assess the performance of various prototypes without having to physically build them is described. By way of example, the techniques are illustrated with results obtained from the computational model of the louvre fin coil which remains as the performance benchmark. The succession of computational models developed was validated by comparison with the measured experimental results of corresponding prototypes wherever these exist.

A variety of alternative heat exchanger prototypes has been developed, fabricated and tested. One of these is the Tube Mesh Heat exchanger which consists entirely of tubes arranged in a turbulence generating grid and is examined in Chapter 5. The purpose of this experiment is to establish the effectiveness of homogeneous turbulence in increasing heat transfer. The results are compared to those of the standard commercial radiator coils pertinent to this study.

The succession of Tube Strut heat exchangers which consist of tubes and interconnecting struts arranged to form parallel plate arrays has been assessed in Chapter 6. Various strut thicknesses and strut spacings have been examined using flow visualisation. Corresponding full scale prototypes have been fabricated and assessed in the coil test rig. In addition each of these arrangements has been compared with a corresponding numerical analysis, serving to validate each particular computational model. Having sufficiently validated the models, the numerical analysis was extended to estimate the effect of varying geometrical parameters, specifically the strut chord length.

A prototype coil having a fin surface with a delta-winglet pair arranged in a Flow-Up configuration is experimentally assessed in Chapter 7. The delta-winglets are positioned directly in front of each tube which is a heretofore untried configuration. The coils are assessed and compared to the benchmark louvre fin coil. In order to investigate other delta-winglet configurations an extensive set of numerical simulations was undertaken. The delta-winglets were arranged in multiples as well as various flow-up and flow down schemes. Although the outcome did not produce a configuration that is overtly superior, the development of this computational model has enormous investigative benefits.

This numerical model has been adopted to assess the potential of a fin surface having a louvre fin and delta-wing combination. Several delta-wing profiles and incident angles are examined in combination with the standard louvre fin surface and the results are reported in Chapter 8.

In order to place the results of the various studies in perspective, the optimisation of the standard louvre fin surface was numerically attempted. Variations in louvre angle

as well as louvre pitch have been assessed. Furthermore the affect of serrating the louvre edges is investigated. These assessments are reported in Chapter 9.

Chapter 10 contains a brief summary of the major results and findings, and suggestions for future work are also given.

Chapter 2

Background Literature

2.1 Introduction

In pursuit of an understanding of factors contributing to the airside heat transfer coefficient of the conventional tube-fin heat exchanger, this chapter is structured to categorise the various geometrical parameters relating to the performance of conventional heat exchangers. Research relating to fin spacing, tube arrangement and the number of rows, as well as tube shape and size is reviewed as a foundation for establishing the underlying principals of the airside heat transfer performance.

There have been numerous varieties and combinations of methods adopted over the years in order to improve the air-side heat transfer coefficient. Some of these methods involved employing metal strips or intricately woven wire fins wrapped around tubes forming so called "finned tubes". Others involved modifying the surface of the continuous plate fins. In the case of the latter, this broad range of techniques employed to achieve such improvement has given rise to the term *enhanced surface heat exchanger*. Most of these involve manufacturing protrusions in the fin surface, resulting in dimpled and waffled fin surfaces. Then incisions were made in the fin surface to create the slit, offset slit, and louvered surfaces. The louvered fin is now widely accepted as the preferred method of obtaining the most compact heat transfer surface, as in addition to improved airside heat transfer performance, the manufacturing process can be achieved using an inexpensive rolling process.

More recently, there has been some interest generated in the use of triangular punched protrusions known as a Delta Wing or pairs of Delta winglets[1], as it is

[1] Note that a Delta-Wing is like an isosceles triangle mounted symmetrically to the flow, and the angle of attack is measured between the plate and the lean of the Delta. A Delta-Winglet

believed that this technique has the potential for even greater improvement. These various surface types are reviewed and compared in some depth as an aid to the understanding of the heat transfer dynamics resulting from the fluid flow as well as boundary layer development on the various fin surfaces. This is done in the context of their associated effects on pressure drop, and where possible, manufacturing feasibility and costs.

Also, any novel or alternative type exchanger designs, which may perhaps have been developed to cater for a particular application, have been assessed for any potential relevance to the current project. This category includes heat exchangers such as the "pin fin", "fine wire", "evaporative film" or "compact" heat exchangers. A compact heat exchanger has been somewhat arbitrarily defined as having an area density greater than 700 m^2/m^3.[2] Area density is the ratio of heat transfer surface to heat exchanger volume. Generally, tube-fin heat exchangers fall into this category and are also called compact, although in some cases the definition as described above may not necessarily apply.

2.2 Factors relating to airside heat exchanger performance

Clearly it is the airside heat transfer resistance which is the limiting factor in the performance of tube-fin heat exchangers. In typical applications the airside resistance generally comprises 90% of the total thermal resistance[3]. In this regard significant efforts are being made to improve the airside performance, usually by the application of fin surface enhancement mechanisms. However, it is important to understand the general thermal hydraulic characteristics of plain tube-and-fin heat exchangers, so that the subsequent interaction of additional flow enhancement devices can be appreciated.

---

on the other hand is like a right-angled triangle(or half delta) mounted perpendicular to the plate, but at an incident angle measured parallel to the inlet flow.

[2] This value applies to units operating in gas streams. For liquid or 2-phase streams, the value is in excess of $300 m^2/m^3$.

2.2.1 Geometrical Considerations

Essentially a tube-fin heat exchanger consists of a bank of tubes which are inserted perpendicularly through a stack of flat heat conducting fins. The ends of the tubes extending beyond the fins are connected with u-shaped bends to facilitate various circuiting configurations. Alternatively the tubes are manifolded at either end to produce a single circuit. The tubes typically carry water or refrigerant, and thus form the water (or refrigerant) side of the heat transfer process. Air is drawn over the fins and outside of the tubes to form the airside heat transfer process.

Perhaps the best place to start in the analysis of factors affecting the airside performance of tube fin heat exchangers is to deal with those having plain fins. Apparently, the plain fin configuration is still the most popular fin pattern, owing to its simplicity, durability and versatility. Here, one can evaluate the effects of the tube diameter and geometry, fin spacing and thickness, as well as the number of tube rows.

2.2.1.1 Tube geometry

In this section the effect of tube diameter is briefly discussed, but more importantly the performance of a staggered tube arrangement as opposed to the aligned tube arrangement is compared.

Traditionally, heat exchangers for HVAC applications have used larger tube diameters, 9.52mm, 12.7mm and 15.8mm. In modern applications the tube size is generally less than 10mm and the longitudinal and transverse pitches are getting smaller. Recently the use of even smaller tubes, 7.94mm and 7.0mm, is becoming popular in residential applications. According to Wang[13], the benefits of using smaller diameter tubes includes smaller form drag caused by the tube, higher heat transfer coefficients due to smaller hydraulic diameter, and less refrigerant inventory into the system. The use of smaller tube diameters coupled with smaller tube pitches results in more compact fin-and-tube heat exchangers.

Wang and Chi[14] performed a series of experiments to establish correlations accounting for variations in tube diameter. Their results indicated that for 2 row coils, the heat transfer coefficients for a tube collar diameter D_c of 8.51mm are slightly

greater than for D_c of 10.23mm. In addition the pressure drop of the larger diameter tubes is 10-15% higher than the smaller diameter tubes. The larger diameter tubes may increase the ineffective area behind the tubes. However, this result is reversed for 1-row coils, and the larger diameter tubing exhibits slightly higher heat transfer coefficients. Wang and Chi's explanation for this is that the ineffective area behind the tubes for a one-row coil is comparatively small. However, as shall be seen in the following section, the stagnant flow zone behind each preceding row tends to be suppressed by the following row. Therefore one would expect the ineffective area of a multi-row coil to be proportionally less than for a single row coil. Using this reasoning, it follows that for smaller tube diameters, the effects of the subsequent rows in suppressing the wake zone is less pronounced, hence proportionally larger wake zones may occur.

One overt distinction in the circuiting of heat exchanger coils is the arrangement of the tubes to be either in-line or staggered. It is commonly accepted that a staggered arrangement results in higher heat transfer capacity, but the reasoning behind this belief has not been formally quantified until fairly recently. A series of heat transfer measurements conducted by Ay et al [15] has produced some insightful and illustrative results differentiating between the merits of the two alternatives. Ay and his team used a reasonably new technique known as infrared thermography to measure local temperatures on a scaled up model of a plate fin surface, with tubes arranged in either an in-line or staggered array. This technique is advantageous in that it has high spatial and temporal resolution, high sensitivity and is non-invasive. They took a thermal footprint of each model surface for varying frontal air velocities at ambient temperature, while maintaining an outside tube temperature of 60°C. They then used this information to derive local heat transfer coefficients h by means of a control volume based finite difference formulation. The details of the technique can be obtained from the original reference and are not pertinent here. Instead, the results of this analysis which bear relevance to the current topic is discussed.

Figure 2.2.1 a) and b) are a selection of graphical results obtained by Ay et al, of their temperature measurements and heat transfer coefficient derivations. At the leading edge of the plate-fin the temperatures are lower and the corresponding heat transfer

coefficients are higher, with this result being more pronounced for the staggered arrangement. For the first two rows, high temperature gradients in front and at the sides of the tubes can clearly be seen, while a gentler temperature gradient is evident at the rear of the tubes because the airflow is swept down stream into the wake. A different characteristic occurs after the third row due to an additional exit effect. For the staggered tube arrangement, the wake behind each tube is somewhat smaller than for similar in-line arrangements. In general it is apparent that the average fin surface temperature of the staggered arrangement is higher, while for the in-line arrangement, the flow channels between the tubes, resulting in high temperature regions in the tube wakes. This resulted in the average heat transfer coefficient of the staggered arrangement being 14-32% higher than that of the in-line configuration.

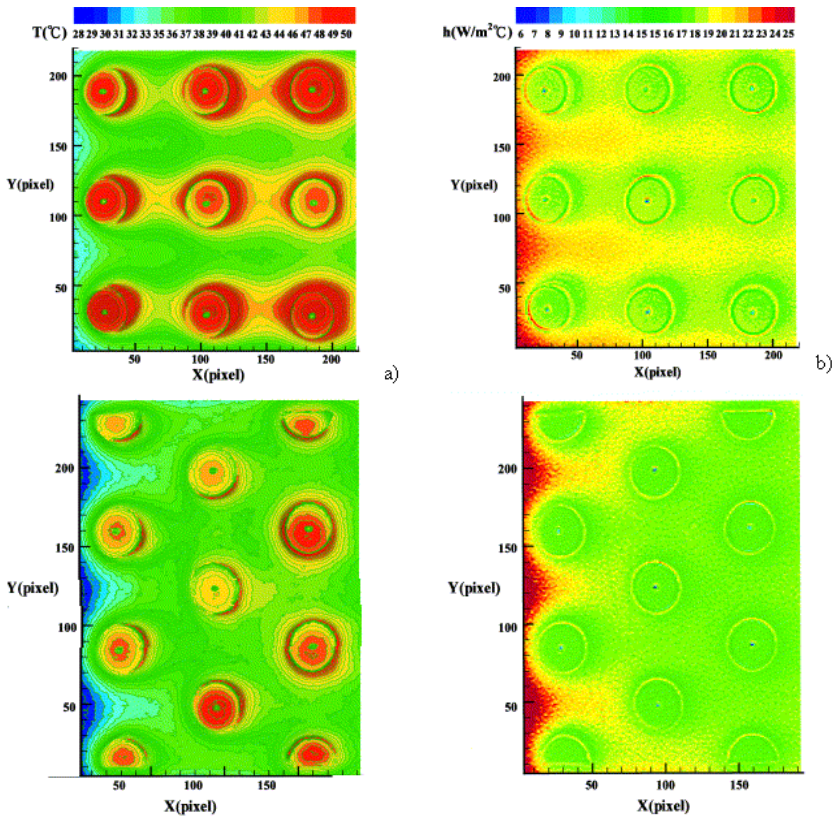

Figure 2.2.1 a) Measured steady state temperature distribution and b) Calculated local convective heat transfer coefficients, on the plate-fin surface at a model fin spacing of 10mm and frontal velocity of 1.0m/s from left to right [15]

2.2.1.2 Number of Tube Rows

An extensive investigation of the performance of various fin configurations, conducted by Lozza and Merlo[12], was carried out in the Luve Contardo[3] experimental facilities. Their aim was to enhance the heat transfer capabilities of air cooled condensers and liquid coolers, and therefore is directly relevant to our current intention of optimising industrial radiators. They assessed the performance of 15 coil prototypes having the same tube and fin geometry but different surface geometries, transitioning from flat, to wavy, to louvered and finally to punched winglets[4].

Lozza and Merlo found that for two rows, successively better results are obtained with fins having increasing degrees of surface enhancement, particularly at higher air velocities. For three rows, the same results were obtained at a high air velocity, although the percentage performance gain from plain fins to louvred fins is reduced. At half the air inlet velocity, all the fins have approximately the same capacity. Evidently, the higher-pressure loss of louvered fins yields to reduced air-flows (much more with three rather than two rows), with a subsequent reduction in *LMTD*, counterbalancing the effect of the higher heat transfer coefficient. For four rows, all louvred fins have the same performance at the high inlet air velocity, but are outperformed by the wavy fins at half the air velocity. They noted when comparing three to four rows, at half the air velocity, that capacity does not increase for wavy fins, and actually decreases in the case of the louvred fins. Even at the high air velocity, there is only a slight increase in capacity in the case of the louvred fins, while there is a significant increase exhibited by the wavy fins. This is because the wavy fins produce less pressure drop, and the airflow remains high. Thus the effect of tube rows has a significant impact on capacity, with 3-rows seeming to have the best average increase, while the selection of 4 rows definitely results in a less desirable design. One further comment is that the capacity did not vary significantly with change in frontal area for all the various enhanced surfaces tested.

---

[3] Luve Contardo is a major European manufacturer of air condensers, evaporators and liquid coolers.

[4] Lozza and Merlo's findings relating to louvred fins and delta winglets are discussed in more depth in section 2.2.2.8.

Referring once again to the results of Wang and Chi[14], however this time considering the effect of the number of tube rows, which they varied between 1,2 and 4 respectively, while maintaining the fin pitch at 1.2mm. The Colburn j factors decrease with the increase in tube rows for Re_{Dc} <3000, but the effect of tube row diminishes as the Reynolds Number increases over 3000. This phenomenon is similar to the test results reported by Rich[16] and Wang et al[17]. At higher Reynolds region, the airflow and temperature distribution inside the heat exchanger may easily become unsteady due to vortex formation and shedding. Hence higher heat transfer performance is seen, and eventually the effect of the number of tube rows on the heat transfer coefficient becomes negligible. As the Reynolds number is decreased, the effect of downstream turbulence tends to diminish (more so with increasing row number). As a result, significant degradation of the heat transfer performance is observed for Re_{Dc}< 3000. This result however, does not apply if the fin pitch is increased. For a fin pitch of 2.2mm, Wang and Chi's results indicate that the effect of tube row on heat transfer performance at low Reynolds numbers is almost negligible. Similarly, they found that irrespective of fin pitch, the friction factors for multiple-row coils are independent of the number of tube rows.

Rich[16] performed another experiment where he took 4 one-row coils and mounted them in series to form a 4-row coil so that the individual contributions from each could be apportioned. Comparing the row-by-row heat transfer coefficients with those of a multi-row coil, he found that the individual row contributions were the same as for a corresponding row of a multi row coil. This not only verified the accuracy of his data, but also proved that the addition of rows downstream has a negligible effect upon heat transfer from the upstream rows. Furthermore, he found that at low Reynolds number, the contribution from each succeeding row to the total heat transfer performance diminishes in the direction of the airflow, while at high Reynolds numbers this trend is reversed. He concluded that the average heat transfer coefficient for a deep coil might be higher or lower than for a shallow coil depending on the Reynolds number.

2.2.1.3 Effect of Fin Spacing

Fin spacing is obviously one of the most important parameters to be considered in heat exchanger design, and too many or too few fins per unit length can be expected to have an adverse affect on performance. It follows that there is an optimum fin spacing with respect to heat transfer and pressure drop.

The effect of fin spacing (s) on the tube fin performance characteristics is complicated by the number of tube rows, as was shown in the previous section. Hence it is useful to consider the case of a single row coil to begin with. Romero-Mendez et al[18] undertook such a study in their investigation of plane fin and tube heat exchangers. They anticipated, based on Hele-Shaw's observations[19], that at small fin spacing the flow streamlines are analogous to those for potential flow over a cylinder; conversely at infinite fin spacing, the flow is that around a cylinder. Thus the flow characteristics of a plate fin and tube heat exchanger, lie somewhere between these extremes. The flow at a single cylinder plate junction has been analysed by Baker[20, 21]. However the geometry of a plate-fin heat exchanger corresponds to a cylinder of finite length bounded by two plates so that the flow characteristics at each cylinder-plate junction can interfere with each other. The hydrodynamics of this type of flow have been studied by Bossel and Honnold [22], where the presence of multiple horseshoe vortices was observed at higher Reynolds numbers.

In addition, Romero-Mendez[18], performed flow visualisation using a variety of techniques, as well as conducting a series of numerical computations. The result of his flow visualisation is graphically depicted in Figure 2.2.2, which shows the development of a horseshoe vortex at the front of the tube as the fin spacing is increased. Note that the flow is characterised by a non-dimensional fin spacing given by $S=s/d$ where s is the fin spacing, and d is the tube diameter. He also observed that at small fin spacing, the flow around the tubes does not separate and it resembles that of Hele-Shaw flow, as he initially anticipated.

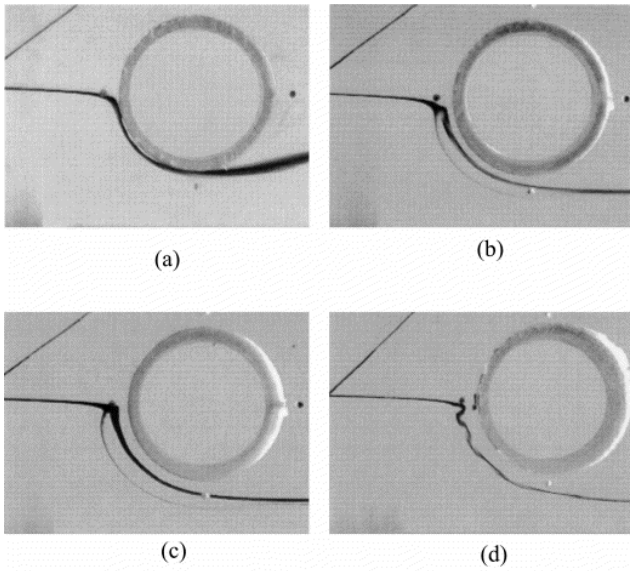

Figure 2.2.2 Horseshoe vortex visualisation for varying fin spacing S=a) 0.116, b) 0.190, c) 0.265 and d) 0.365 [18]

He further observed that although the flow is laminar (since it is characterised by the Hele-Shaw limit), the heat transfer is not limited by the presence of a stagnant wake zone. This initially appears as a closed recirculation bubble as the fin spacing is increased and separation takes place, until the width of this wake region covers the entire backside of the tube. On further increasing *S,* a point is reached where the recirculation region begins to communicate with the downstream flow, and eventually there is a reverse re-entrant flow towards the tube. This re-entrant flow would be expected to provide good heat transfer at the back of the tube. He had good agreement with his computational results as far as the shape of the recirculation zone is concerned, although comparison is not possible when the wake becomes unsteady due to the complexity of the numerical modelling required. His numerical study involved the calculation of Nusselt number distribution on both the fin surface and the tube surface, and his results are illustrated in Figure 2.2.3.

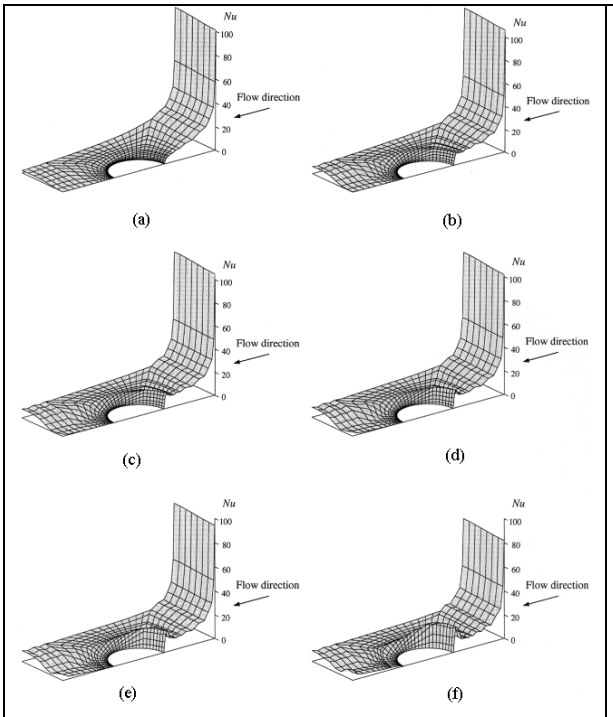

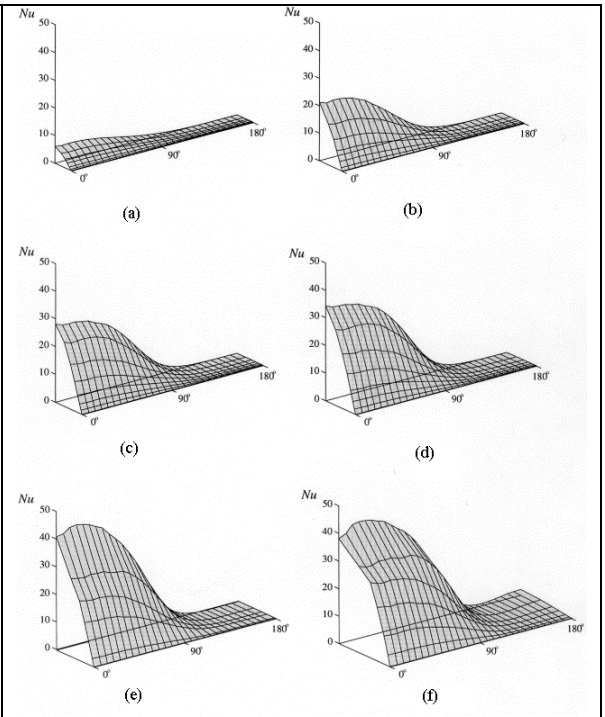

Nu over fin surface	Nu over cylinder surface

Figure 2.2.3 Nu distribution for Re=630 and varying S a) S=0.116 b) S=0.165 c)S=0.190 d) S=0.125 e) S=0.265 and f)S=0.365 [18]

These plots of Romero-Mendez's numerical calculations of *Nu* show a similar pattern to that found by Saboya and Sparrow[23]. They used the Napthalene sublimation technique to measure local heat transfer coefficients on two fin surfaces separated by a single tube row. Observations of the naphthalene fin surfaces after a test run at a Reynolds number of 1271, identified two semicircular erosion patterns upstream from, and wrapped around the base of the tube indicative of the presence of two horseshoe vortices there. This resulted in two corresponding peaks in the *Nu* values just upstream from the tube. At a Reynolds number of 648, only one horseshoe erosion pattern and hence one peak in the Nusselt number was observed. This pattern is also clearly observed in Romero-Mendez's numerical plot of *Nu* over the fin surface at a Reynolds number of 630, shown in Figure 2.2.3**.** His three dimensional plots make it possible to easily visualise the spatial variation in *Nu* over the fin and tube surface, while although the results of Saboya and Sparrow were essentially the same, their results presented in a series of two dimensional graphs makes visualisation awkward.

Studying Figure 2.2.3 it can be seen that the region of highest *Nu* is at the leading edge of the plate where the thermal boundary layer is thin. Regrettably, in conventional tube fin heat exchanger designs, this feature cannot be exploited since the heat driving potential is typically small in this zone. Although the region of highest *Nu* is at the leading edge of the plate where the thermal boundary layer is thin, this is not useful for heat exchanger purposes since it has been shown that the heat flux falls sharply there on taking fin efficiency into account[5]. For the smallest fin spacing there is no region of high *Nu* ahead of the tube but as *S* increases a peak appears directly in front of the tube due to the presence of a horseshoe vortex there. At small *S* values there is no vortex system present upstream of the tube because the vortex systems due to the two fins cancel each other out. Note that the heat transfer from the front of the tube becomes progressively more important as *S* and the tube area increases. The smallest values of *Nu* for all *S* are directly behind the tube, this being a region that does not directly participate in heat transfer.

Romero-Mendez also plotted the overall heat transfer per unit pressure drop per unit length of tube as a function of fin spacing, and found that this showed a maximum. This value gives an indication of the compactness and pumping requirements of the heat exchanger, and this can be optimised with respect to fin spacing. If *S* is too small the pressure drop is high, while if it is large there are too few fins for effective heat exchange.

In summary, Romero-Mendez points out that although his investigation was for a single row heat exchanger, the same results would apply, perhaps to a greater degree for a multi-row device. He argues that the results become less influenced by the entrance region, which is only applicable to the first row, while the subsequent rows are more influenced by the heat transfer around the tubes, which he has shown to be highly dependent on fin spacing.

It appears that the effect of fin spacing is influenced to a considerable degree by the number of rows. Wang and Chi[14] found that depending on the number of tube rows,

---

[5] It should be noted that Saboya and Sparrow, and Romero-Mendez used or assumed an isothermal fin surface for their measurements and computations respectively. This assumption may only be valid, if the fins have a large thermal conductivity, or have a large thickness.

the heat transfer characteristics were strongly related to the fin pitch. They found that for N=1 or 2, the heat transfer performance increased with decrease in fin pitch. For $N \geq 4$ and $Re_{Dc} > 2000$, the effect of fin pitch on heat transfer performance was negligible. They also found that for the same fin pitch, the effect of the number of tube rows on friction performance was very small. These findings were similar to those previously reported by Rich[24] and later Wang et al[17], who concluded that the heat transfer coefficients were essentially independent of fin spacing for a 4-row configuration. Furthermore, in an analogous series of tests, Wang et al[25] concluded that the effect of fin pitch on the heat transfer performance is also negligible for multi-row louvred and wavy fin surfaces. However for a 1-2 row configuration, Wang and Chi[14] found that the heat transfer performance shows a detectable dependence on fin pitch. For $Re_{Dc} > 5000$ the effect of fin pitch is negligible. For $Re_{Dc} < 5000$ the heat transfer performance increases with decrease in fin pitch, especially for N=1. Wang and Chi explained this by referring to the numerical results of a study on the effects of fin pitch carried out by Torikoshi et al.[26]. They conducted a 3D numerical investigation of a 1-row plain fin-and-tube heat exchanger; a schematic of their results is plotted in Figure 2.2.4.

Torikoshi *et al*[26], investigation showed that the vortex that forms behind the tube can be suppressed and the entire flow region kept steady and laminar when the fin pitch is small enough as in (a) where S=0.17. Increasing the fin pitch would lead to a noticeable increase of the cross-stream width of the vortex region as shown in (b) where S=0.3, resulting in lower heat transfer performance. Although there is similarity at smaller fin spacings between these simulations, and those of Romero-Mendez discussed earlier, there is a departure in agreement at larger fin spacings, because Romero-Mendez's modelling included the beneficial effects of a system of horseshoe vortices appearing at the front of the tube and enhancing the local Nu numbers in this region. Figure 2.2.4(c) simulates how the addition of a tube row tends to stabilise the flow behind the first row, minimising the wake area so that the effects of fin spacing are less profound.

Figure 2.2.4 Schematic illustration of 3D computational results for the effect of fin pitch (taken from Torikoshi et al[26])

Yan and Sheen[27] carried out extensive experimental investigations of the influence of fin spacing and tube rows for plain, louver and wavy fin configurations. They varied fin pitch between 1.4, 1.69 and 2.0mm and varied the tube rows from 1 to 4 inclusive. This gave 12 samples for each fin type, totalling 36 samples altogether. For the plain fin configuration, he found that both the j and f factors increase with the *decrease* in fin pitch, but for louver fins, the effect of fin pitch did not show a trend. They also compared heat transfer coefficient h with fan power, and found that in general h is highest for the minimal tube row number ie N=1. Furthermore, compared with plain and wavy, the louver fin surface shows the highest h overall, meaning that the louver surface is relatively most advantageous when used at the same operating condition. They then used a volume goodness comparison VG-1 criteria as defined by Webb[28] which measures the possible reduction in surface area required for fixed values of fan power, heat duty and temperature difference. They found that up to a 40% reduction in surface area was obtainable using a louver fin surface relative to a plain surface, and this area reduction increases with the *increase* in fin pitch.

2.2.1.4 Effect of Fin thickness

The literature available on the effect of fin thickness on the thermal-hydraulic characteristics of the plate fin-and-tube heat exchanger is minimal, and very few experiments have been conducted to investigate this parameter.

Wang et al[17], did a review of the existing literature on this aspect leading to the following remarks:

> "Gray and Webb argued that fin thickness should not affect heat exchanger performance. They explained that the fin thickness affects only the airflow velocity in the heat exchanger, which is accounted for by the Reynolds number. In addition, the friction correlation excludes the entrance and exit losses. As a result, it is likely that the fin thickness may not affect the thermal-hydraulic characteristics of the plate fin-and-tube heat exchanger. On the contrary, Briggs and Young proposed a heat transfer correlation for individually finned tubes, which included a term for the fin thickness $t^{-0.11}$, which implies that fin thickness has a slight affect on heat transfer coefficients. Rabas et al developed more accurate *j* and *f* correlations for low fin height and small fin spacings, and their heat transfer correlation showed a similar dependence on fin thickness. In general it appears that the influence of fin thickness on the thermal hydraulic performance of tube-fin heat exchangers is small."

Wang et al[17] performed a series of experiments which measured the effect of fin thickness. In this study they included 15 coil samples and used fin thicknesses of 0.13mm and 2.0mm. Using the same correlation as was determined by Briggs and Young, their data indicated that the exponent dependence of fin thickness is even smaller than 0.11. They concluded that fin thickness has negligible effect on both heat transfer and friction characteristics of plate tube-fin-heat exchangers.

2.2.2 Fin Surface Enhancement

It has been shown experimentally by Gilbert[29] that the flow in a plate-fin coil (ie with plain fins), remains laminar at all points, even at velocities of 6m/s, and having 6fpi. The fin spacing at 6fpi is relatively wide considering today's high performance radiator coils having 9-15fpi. Since laminar flow is undesirable from a heat transfer perspective, fin surfaces are modified in an attempt to disturb the flow.

Enhanced fin surfaces are attractive from an application point of view because better performance can be obtained without affecting production costs (apart from a limited increase in pressing tool investment cost). However, better heat transfer performance is obtained at the expense of unavoidably higher friction losses. In fact, more often than not, the increase in the pumping power is greater than the increase in heat transfer, because only part of the increased turbulence is effective in promoting heat transfer; the balance is wasted in ineffective eddies according to Fraas[30].

There are numerous types and combinations of fin surface enhancement methods that have been attempted in order to improve the airside heat transfer coefficients of tube-fin heat exchangers over the years. Figure 2.2.5 has been reproduced from Shah et al[31], and displays a sample of just some of the earlier surface enhancement features used on plate fins. Although the earlier methods appear to have been indiscriminately generated, currently, along with more contemporary techniques, they can be categorised into three successive generations of fin surface enhancement.

Figure 2.2.5 Continuous fins on an array of round or flat tubes [31]

The first generation of fin surface enhancements are those that are superimposed on a continuous fin such as smooth wavy, herring-bone wavy or dimpled surfaces. These work by causing sudden direction changes to the gas so that locally, the temperature and velocity gradients are increased, causing local enhancement of both heat transfer coefficient and friction factor. There exists the likelihood of separation occurring on certain parts of the surface, and here the heat transfer coefficients will be low and the pressure losses high.

The second generation of fin surface enhancements result in discontinuations in the fin surface such as slit fin or louvred surfaces, where the airflow direction change is kept to a minimum. These interrupted surfaces feature enhanced heat transfer mechanisms such as boundary layer restarting, wake management and flow destabilisation. A recent patents review by Wang[32] and a comparative study by Wang et al[13] have outlined many of these interrupted fin surfaces.

It is believed that the third generation of fin surface enhancements can improve heat transfer performance without the excessive pressure losses associated with interrupted surfaces. These surfaces employ longitudinal vortex generators such as delta winglets that provide swirling motion to the flow field. Longitudinal vortices have their axes parallel to the main flow direction and it is believed that they are more effective than transverse vortices from a heat transfer perspective. Note that the typical horseshoe vortex generated at the tube fin junction of plain tube fin surfaces is an example of a transverse vortex.

2.2.2.1 Wavy or Waffle Fins

A great majority of tube-fin heat exchangers used in HVAC applications have wavy or waffle fins. The fins are rippled in the vertical direction, and along the leading and trailing edges. Contrary to a widely held belief, this is not done to promote turbulent flow, and the flow remains laminar regardless of the ripples. The vertical ripples provide stiffness and increase the surface area, while the leading and trailing edge ripples serve to minimise impact damage. Apart from these practical advantages, the wavy fin surface, compared with a plain fin surface, can lengthen the air flow inside the heat exchanger and cause better mixing of the airflow and consequently better

heat transfer can be expected albeit at disproportionately greater pressure drops. In general the percentage increase in pressure drop can be anywhere between 2 to 10 times the percentage increase in heat transfer. In spite of this, wavy fins are still very popular, particularly in refrigeration applications.

A numerical analysis of heat transfer and pressure drop of a wavy fin heat exchanger was conducted by Jang and Chen[33]. In order to verify the validity of their numerical model, they compared their results with the available experimental data obtained by Wang[34] for several fin spacings using the same waffle criteria and heat exchanger geometry, as well as that of a plain fin counterpart. Their numerical results agreed well with their experimental results, and demonstrated that the Colburn j factor of the wavy fin arrangement was higher by 63-71% than that of the plain fin counterpart, while the fanning friction factor f of the wavy fin configuration was higher by 75-102% than the plain fin configuration. In further simulations, they varied wavy height and wavy angle, as well as the tube row number. They concluded that for a fixed wavy height, both Nusselt Number and pressure coefficient increase with increase in wavy angle, while for an equal wavy angle they decreased as the wavy height increased. Note that by geometrical definition, increasing the wavy angle(at a fixed wavy height) or decreasing the wavy height(at a fixed wavy angle), means the wavelength of the wavy corrugations decreases, resulting in more corrugation for a fixed flow length. Therefore the boundary layer is interrupted more frequently. They also evaluated the area goodness factor j/f for each case and found that the greater the number of wavy corrugations for a given flow length, the lower the value of the j/f factor[6]. They also observed that the effect of tube row number on j and f is less important in a wavy fin as compared to a plain fin counterpart.

In an experimental study, Wang et al[34] examined the effects of waffle height on heat transfer and friction characteristics, using a sample of 13 heat exchangers. The waffle heights tested were 1.18, 1.32 and 1.58mm, and 4 plain fin configurations were included for comparison. Their results showed that both heat transfer coefficient and pressure drop are increased as the waffle height is increased, but the pressure drop increase is substantially more than the increase in heat transfer coefficient. Also, these

[6] The implication is that the friction factor increases at a greater rate then the heat transfer, as the number of wavy corrugations increases per unit flow length.

effects are more pronounced at higher air velocities. The heat transfer enhancement ratios h_{wavy}/h_{plain} for a fin pitch of 1.7mm are greater than those for a fin pitch of 3.1mm. Their results are summarised in Table 2.1.

Table 2.1 Percentage increase in heat transfer and pressure drop of wavy fins over plain fins [34]

		% Increase over plain fins			
Frontal Velocity m/s -->		2.5 m/s		5.6 m/s	
Waffle Height	Fin Pitch	*h*	ΔP	*h*	ΔP
1.18 mm	1.7 mm	4.5	38	-	-
	3.1 mm	0	15	4	32
1.58 mm	1.7 mm	24	60	45.4	78
	3.1 mm	0	20	15	68

Considering the percentage increase in *h* over plain fins at 2.5m/s as documented in Table 2.1, one can observe that for larger waffle heights, the percentage improvement is strongly dependent on fin pitch, while for smaller waffle heights the effect of fin pitch is not so pronounced. An improvement of 24% and 4.5% respectively, is obtained at the smaller fin pitch. At the large fin pitch there is no heat transfer improvement at all irrespective of waffle height, however there is still a 15-20% increase in pressure drop.

Their explanation for this can be appreciated by referring to Figure 2.2.6, which schematically illustrates the effect of interwall spacing on flow patterns. As seen in Figure 2.2.6(a), in the case of the larger waffle height and smaller fin pitch, the airflow across the heat exchanger is directed by the corrugation, which may effectively reduce the size of the recirculation zone, hence higher heat transfer is expected. As the fin pitch is increased, the separation zones expand; and lower heat transfer is expected. On the contrary, for a small waffle height as shown in Figure 2.2.6(b) there is no significant difference in the recirculation zones as the fin pitch is increased.

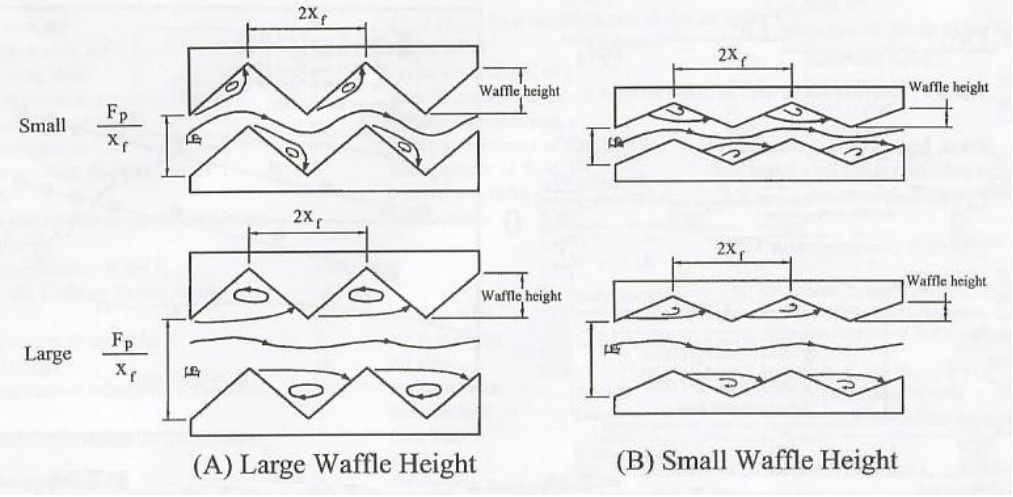

Figure 2.2.6 Pattern of fluid flow in a corrugated channel of varying width and corrugation heights [34]

Wang et al[34], report further that the numerical flow simulation for a corrugation channel by Ramadhyani[35] depicted analogous results. Ramadhyani's results indicate that for a smaller corrugation angle Θ=15°, there is no appreciable heat transfer augmentation. He suggests that to obtain an appreciable heat transfer enhancement, the corrugation angle should be at least 20°.

2.2.2.2 Slit and Super Slit Fins

Interrupted surfaces such as slit fins provide enhancement of the air-side heat transfer coefficient by the repeated growth and destruction of the laminar boundary layer, on successive leading edges. The advantages of a leading edge boundary layer development are immense. The leading edge effect on localised heat transfer has been dramatically reinforced through a number of investigations. The variation in heat transfer coefficient with distance from the leading edge of a flat plate is shown schematically in Figure 2.2.7, which has been reproduced from Mills[36]. The diagram implies that the heat transfer coefficient is infinite on the leading edge. Therefore boundary layer restarting is of exceptional benefit with respect to heat transfer enhancement. Of course, to capitalise on this feature, it is necessary to ensure that the leading edges are located where there is sufficient temperature gradient to ensure adequate heat exchange can occur. Ideally areas of high temperature gradient as well as high velocity gradient should overlap.

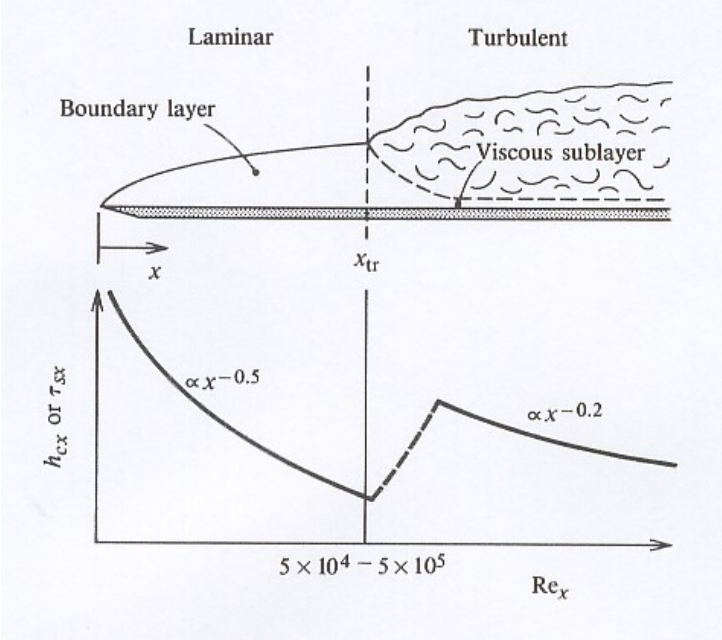

Figure 2.2.7 Sketch illustrating the variation in heat transfer coefficient h and shear stress τ along the length of a continuous fin [36]

Of course louvred surfaces also fall into the category of interrupted surfaces, but unlike slit surfaces, they impose a directional shift in the flow, which may increase turbulence, but may also produce relatively higher pressure drops than slit fins may. They measured and compared the performance of two super slit surfaces, and a louvred surface against that of a plain surface. They were careful to choose the fin surfaces so that in all cases (apart from the plain fins) the extent and shape of the interrupted area in plan, was very similar. It also appeared that the cross sectional height of the interruptions, were similar in all cases as well. Their results indicated that both of the slit surfaces increased the j factor over the plain surface by a greater amount than that of the louvred surface. On the other hand, the louvred surface increased the f factor over the plain surface by a greater amount than the two slit surfaces. This clearly demonstrates the benefits of slit fins over louvred fins, at least with respect to this selection of fin surfaces.

Wang et al[37] commented on a flow phenomenon which is peculiar to slit fin surfaces. The arrangement of the slits in combination with those in adjacent fins form a parallel plate array as schematically illustrated in Figure 2.2.8, which compares the airflow

patterns through a louvre and slit fin geometry[7]. They draw on the recognition that these interrupted surfaces may cause vortex shedding above a critical Reynolds number, and that the self-sustained flow oscillation associated with vortex shedding can enhance heat transfer[8].

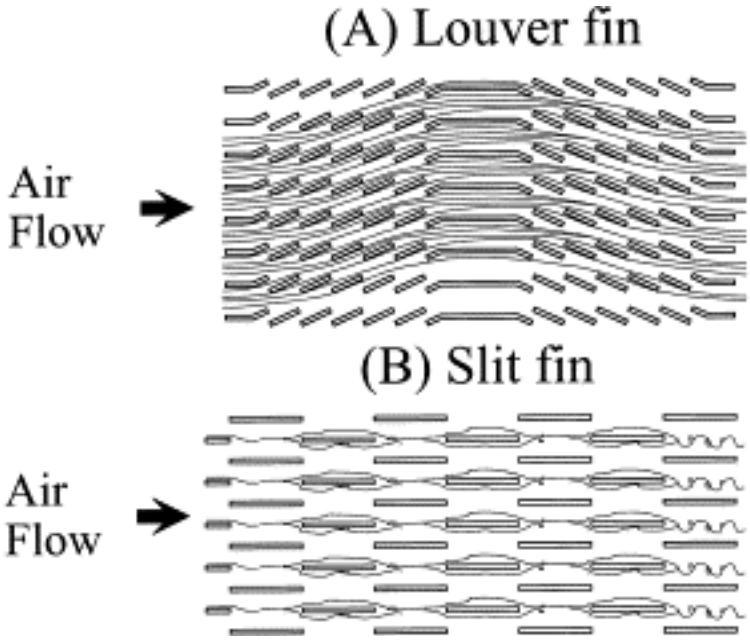

Figure 2.2.8 Schematic of the airflow pattern of the slit fin and louvre fin geometry [37]

It is evident that the performance of slit fins is strongly dependent on the fin spacing, in conjunction with the number of tube rows. Wang et al[37] tested various slit fin surfaces encompassing 3 groups of fin pitches of approximately 1.2, 1.7 and 2.5mm. Their results showed that the heat transfer performance increased with decrease in fin pitch for N=1, however for $N \geq 4$ the effect of fin pitch on heat transfer was reversed. In addition to the effect of fin pitch, the heat transfer performance decreased with the number of tube rows while the friction factors were relatively independent of the

[7] The slit fin geometry can be considered as a louvre geometry with a louvre angle of zero ie parallel louvres.
[8] A more detailed discussion on Parallel Plate Arrays can be found in Section 2.4

number of tube rows[9]. They also performed a comparison of j and f factors at fin pitches of 1.2 and 2.5mm and with tube rows varying up to 6 rows. For both fin pitches the effect of the number of tube rows diminishes as the Reynolds number increases over 2000. This is because the vortex developed in the upstream was shed to the downstream and caused good mixing of the flow. At a fin pitch of 1.2mm they noted that the heat transfer performance dropped sharply at a tube row of 4 and 6. They attributed this to the "wake-effect" of the slit fin, which manifests due to a velocity deficit and temperature excess existing in the wake of each fin which may reduce the effective heat transfer characteristics. They explain that the "wake effect" may accumulate from the upstream and cause "un-recovery" phenomenon at the downstream. This phenomenon is especially pronounced with further increase of the number of tube rows (large number of slits) and offsets the contribution of vortex shedding.

In an experimental study carried out by Du and Wang[38] it was found that for the number of tube rows N=1, heat transfer increases with decrease in fin pitch. However, for N>2 this effect is reversed. Furthermore, for Re_{Dc}<1000 heat transfer performance decreases significantly with the number of tube rows. For Re_{Dc}>2000 the heat transfer performance is relatively insensitive to change with the number of tube rows. They also found that the friction factors are relatively independent of the number of tube rows.

In a subsequent study Wang et al[13] also concluded that the effect of tube row on frictional performance of slit fin geometry is relatively small, and the influence of fin pitch on heat transfer performance is also relatively small for Re_{Dc}>1000. More importantly, they found that the breadth of the slit plays a significant role in improving the heat transfer performance, in comparison to the effect of slit height. Their results indicated that the heat transfer performance could be considerably improved by reducing the slit breadth from 2.2mm to 1.0mm. They explain this by referring to measurements obtained by Mochizuki et al who showed that turbulence intensity was increased by between 25-50% by halving the slit breadth. In addition, on

[9] Almost all of the fin patterns reveal these characteristics. Corresponding results were reported by Rich and Wang for plain fins, and by Wang for louvred and wavy fins as mentioned in section 2.2.1.3.

an area goodness and volume goodness basis, Wang et al[13] found that the airside performance of slit fin and louvred surfaces are comparable in all cases tested, and that they are superior to plain surfaces. However, their superiority over plain surfaces at decreased fin pitch and Reynolds numbers may be lost.

2.2.2.3 Offset Strip Fins

Offset strip fins are another example of how the fin surface can be arranged to replicate a parallel plate array in a compact heat exchanger. Offset strip fins form an enhanced fin geometry which, according to Manglick and Bergles[39], is very widely used. The geometry has a high degree of surface compactness, and a substantial heat transfer enhancement is obtained as a result of the periodic starting and development of laminar boundary layers over uninterrupted channels formed by the fins and their dissipation in the fin wakes. An increase in pressure drop due to increased friction and a form-drag contribution from the finite thickness of the fins is understandable. Typically, many offset strip fins are arrayed in the flow direction as shown schematically in Figure 2.2.9.

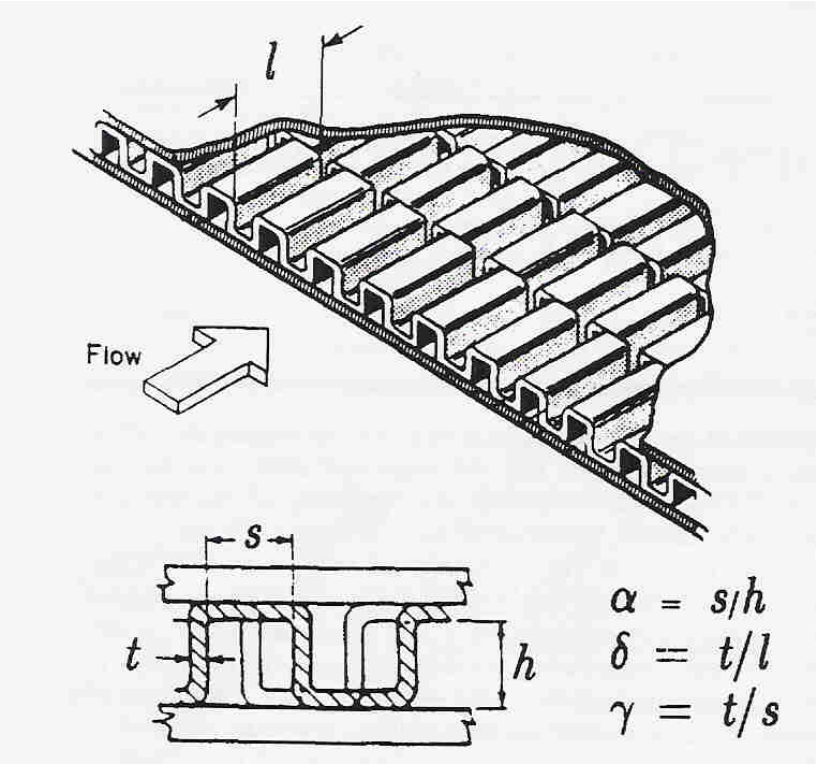

Figure 2.2.9 Example of a typical offset strip fin core [39]

Their surface geometry is described by the fin length l, height h, transverse spacing s, and thickness t. The fin offset is usually uniform and equal to a half-fin spacing, and it is in this arrangement that the resulting geometry in effect forms a parallel plate array. As can be seen from Figure 2.2.9 this type of geometry lends itself ideally to be used in a cross flow application, typically in a plate heat exchanger application, and is not normally considered for a fin and tube arrangement.

2.2.2.4 Elliptical, Serrated and Segmented Fins on Finned Tubes

Elliptic shaped fins have been investigated as it is suspected that there may be an advantage when using elliptic tubes with elliptic fins, due to the reduced form drag of elliptic tubes when compared with round tubes. In an analytical study conducted by Lin et al[40] it was shown that fin efficiencies increase as the axis ratio Ar[10] increased. Elliptic fin efficiencies are up to 4% higher than corresponding circular fin efficiencies having the same perimeter for fully dry conditions, and up to 8% for that of fully wet conditions.

Another variation in annular fins, are those having serrated fins. Fins with crosswise cuts at the fin tip have rapidly been replacing the conventional plain annular fins in heat exchangers such as heat recovery heat exchangers, according to Hashizume and colleagues[41]. This is particularly beneficial for fin materials of low ductility, in applications involving high temperature gasses where ferrous metals are used, which not only have low ductility but also low thermal conductivity. The fin serrations effectively increase the number of fins, and also enhance heat transfer due to turbulence at the fin tip.

Hashizume[42] also performed a comparative study of the performance of spirally wound fins, plain annular fins, segmented fins and finally semicircular fins. The semicircular fins are annular fins in which the downstream half of the fin has been removed. Although variations in pressure drop between the spiral, plain and segmented fins were insignificant, he reports a considerable reduction in pressure drop

[10] Axis ratio Ar of an elliptic tube defined by a/b.

in the case of semicircular fins. His heat transfer comparison showed that the semicircular fins produced the most promising heat transfer coefficients in spite of the reduction in fin surface area. From flow visualisation, he observed that the downstream wake region containing a vortex pair recirculation system became unstable or was not formed when the downstream half of the fin was absent. In a conventional wake recirculation zone it has been shown that the fluid remains for a certain length of time (known as the residence time) and the fluid velocity here is lower than in the main stream. Therefore, the heat transfer coefficient in the recirculation zone is poor[11]. Removing the downstream half of the fin reduces the area of the recirculation zone behind the tube and therefore results in a superior heat transfer performance. Another advantage of so much fin removal, is that the tube pitch can be reduced resulting in a more compact heat exchanger.

2.2.2.5 Louvred Fins

Kays and London[2]were the first to report heat transfer and pressure drop data on louvred fins. These were typically continuous lengths of louvred sheets which were laced between flat tubes, forming triangular or rectangular shaped channels. This arrangement is popular in the automotive industry for radiators and intercoolers. Since then much experimental research has been gathered for the performance characteristics of louvred surfaces arranged in this manner. As a result the thermal characteristics of these louvred surfaces have been identified to a greater degree. For example it has been established by Davenport[12] that at low Reynolds numbers the fluid flow tends to be largely down the ducts between the fins. This gradually changes to almost complete alignment with the louvres as Reynolds number increases. He conjectured that at low Reynolds numbers the laminar boundary layers on the louvres are sufficiently thick to effectively block off the gaps between adjacent louvres in the same fin.

This was confirmed by the finite-difference analysis results of Cowell et al[43]. They proposed that the effectiveness of louvred surfaces is attributed to their ability to

---

[11] This also explains why the heat transfer coefficient in an aligned arrangement is lower than in a staggered arrangement, because not only the downstream side but also the upstream side of the fins in an aligned arrangement lie in the recirculation zone.

[12] Davenport,C.J. reported these findings in his PhD Thesis on *Heat Transfer and Fluid Flow in Louvred Triangular Ducts.*

replicate the "multiple flat plate" behaviour, which is most likely to be achieved if the flow is completely aligned with the louvres. From the results of flow visualisation tests, Webb and Trauger developed correlations to predict the flow efficiency (Φ), which they defined as the ratio of actual transverse distance to ideal transverse distance. The flow efficiency is 1 when the flow is parallel to and through the louvres. It is equal to 0 when the flow is a fully duct-directed flow. This appears to explain why louvred fin surfaces exhibit a distinctive flattening and fall off of the j factor curves at lower Reynolds numbers, as shown in the results of several researchers[44, 45]. Kim and Bullard[46] investigated experimentally the thermo-hydraulic performance of multi-louvred fin and flat tube heat exchangers, by varying louvre angle, fin pitch and flow depth[13]. Essentially they found that the effect of louver angle on heat transfer is different according to flow depth mainly, and Reynolds number, while fin spacing had only a small effect. They found that heat transfer performance decreases with flow depth while pressure drop increases with flow depth. They explain that at the relatively low velocities used, the decrease in heat transfer coefficients in the case of larger flow depth suggests that the boundary layer growth in the duct directed portion of the flow is larger than the effect of adding louvres in the louvre directed portion of the flow. Thus one could argue that in the ideal case of flow efficiency (Φ=1), the heat transfer coefficients would be independent of flow depth. This seems to imply that any perceived benefits of increasing the width of the flat tube are limited.

Having previously reported on the work undertaken by Lozza and Merlo[12], and their findings relating to the effect of the number of tube rows in section 2.2.1.2, further reference is made to their findings on louvred fins. Recall that they experimentally evaluated the performance of coils having various surface enhancements and combinations thereof. Included was an extended louvre surface where the louvre area is arranged closely around the tubes, forming an X-shaped area as can be seen in Figure 2.2.10 which illustrates a sample of the surfaces tested. Their initial work was a comparison of the Colburn j factor and fanning friction factor f at various Reynolds numbers.

[13] The flow depth is geometrically related to the width of the flat tubes.

They found that corrugated fins provide a limited improvement of f and j, with the traditional wavy fin remaining the best out of these. Louvered fins greatly improve the heat transfer coefficient, but incur much higher pressure losses, the amount depending on louvre height. In particular, a louvre height of 0.9mm in comparison to 0.75mm does not improve heat transfer but only increases pressure loss. Presumably this is because a louvre height greater than the boundary layer thickness provides no further disturbance to the boundary layer, but simply begins to throttle the bulk flow. Clearly, louvred fins require a strict dimensional control.

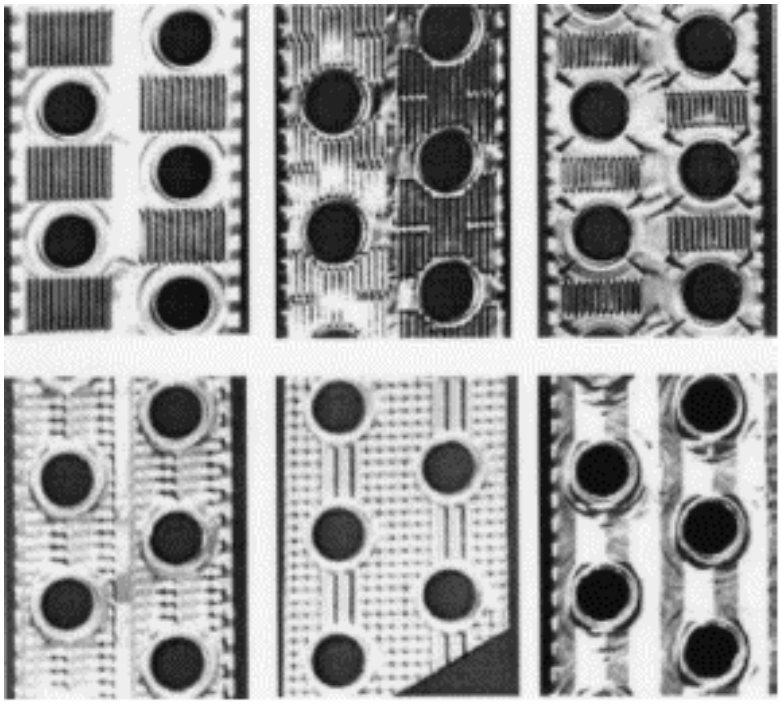

Figure 2.2.10 A selection of fin surface enhancements. The top row consists of various louvered surfaces: conventional on the left, extended in the centre and with winglets on the right. The first two in the bottom row, are the corrugated fins, while the wavy fin is on the right [12]

Also, Lozza and Merlo found that the heat transfer enhancement of louvered fins with respect to wavy fins is larger at lower Reynolds numbers. Once again, this can be explained in terms of boundary layer development. The thicker boundary layers at lower Reynolds numbers have an increased potential to be affected by any flow disturbance. The extended louvre X prototypes provide an exceptionally high heat

transfer coefficient; double that of the wavy fins. Also, the pressure loss is only slightly higher than for the conventional louvre of the equivalent louvre height.

From their comparison of the Colburn j factor and fanning friction factor f at various Reynolds numbers, they were able to select 4 coils with comparable goodness factors defined by j/f but very different values of j and f. They subsequently investigated the outcomes of various design parameters on coil selection such as frontal area and number of rows. They compared these effects on capacity, by plotting this as a function of frontal area for two, three and four row coils using both a 6-pole and a 12-pole motor[14]. Furthermore, they compared their respective performances by evaluating the "*volume goodness factor*" *(GV)* as a function of the "*ideal pumping power*" *(PP)*. They found that at the same pumping power, GV noticeably increases for enhanced fins, even if a lower air velocity is required to compensate for the higher friction factor. This follows from the aspect that PP depends on velocity variation with a 2.5-2.75 power versus a 0.3-0.45 power for the heat transfer coefficient. This implies that a small velocity reduction facilitates a considerable reduction in f with minimal effects on the heat transfer capabilities. Or, according to these indications, it may be advantageous to have a slightly larger front area to take full advantage of enhanced fins without affecting the pumping power. In practice however, the use of enhanced fins would increase the heat exchanger capacity at the same volume and cost. Unfortunately the increased friction factor would reduce the air-flow when coupling the coil to a real, not ideal fan having a given head-flow curve. Also, the effectiveness of louvred fins depends on the louvre height. Beyond a critical louvre height, any further increase does not increase heat transfer, only pressure drop[15].

The louvred fin surface is now widely used in both automotive and residential air conditioning systems. Possibly, one contributing factor to their widespread usage, is

---

[14] Halving the fan allowed the effect of varying flow rates, brought about by the increased friction of the various enhanced fin surfaces, to be compared. The air flow reduction has two detrimental effects: (i) the lower air velocity reduces the heat transfer coefficient, (ii) the air temperature increases while crossing a condenser unit, thus reducing the $LMTD$ at the same initial temperature difference.

[15] This seems to infer that the louvre height can only be optimised for one particular airflow rate. Therefore, fixing of the louvre height should be done at the highest airflow the heat exchanger is likely to encounter. Heat transfer enhancement will still be possible to a lesser degree of optimisation at lower airflow rates, without any additional pressure drop losses.

that louvered fins in comparison to other interrupted fin surfaces, can be manufactured by high-speed production techniques and therefore are less expensive when produced in large quantities, according to Chang and Wang[47]. In automotive applications such as radiators, condensers and evaporators, the louvre fins are generally brazed between flat extruded tubes in a continuous serpentine fashion to form corrugated rectangular or triangular channels. However, in residential air conditioning systems, round tubes are generally used in a block of parallel continuous fins. The general merits of the flat tube arrangement over the round tube configuration are discussed in section 2.2.3.2. In this section it is noted that the heat transfer and friction characteristics of the two alternative arrangements mentioned above are quite different. As mentioned in the preceding paragraph, during the past few decades there have been considerable experimental works devoted to the first type as used in automotive applications. Conversely, for louvre fins with round tube configurations, the airside performance was not available until Wang et al[25, 48]and proposed separate correlations for the fin-and-tube configuration with round tubes. Not surprisingly, they found that, as with the plain fin geometry, the j factors decrease with increase in tube rows for Re_{Dc}<2000, and are relatively independent of tube row for Re_{Dc}>2000. Similarly they found that the effect of fin pitch has negligible effect on heat transfer for Re_{Dc}>1000, although there is a distinctive decrease in the heat transfer performance with decrease in fin pitch for Re_{Dc}<1000. Note that plain fins do not tend to exhibit such a distinctive decrease in heat transfer performance at these lower Reynolds numbers.

2.2.2.6 Louvres with serrated edges

In all louvred surfaces the louvres have straight edges, and this aspect has remained unchanged since they were originally conceived. Serrated louvres can easily be incorporated into the fin surface by using the same manufacturing technique. Considering the advantages of increasing turbulence in tube fin heat exchangers it is ironic that no consideration has been given to the virtues of having interrupted louvre edges. For example by incorporating serrations into the louvre edges, several advantages may be realised. For one, the leading edge length is increased. Also the serrations may generate small scale turbulence which could enhance local heat transfer

upon the louvre surfaces. Therefore this is a geometrical consideration that may prove beneficial and seemingly would be useful to investigate.

2.2.2.7 Delta-Winglets

Turbulence and rotating fluid motions may be classified as transverse and longitudinal vortices. The rotation axis of a transverse vortex lies perpendicular to the flow direction while the longitudinal vortices have their axes parallel to the main flow direction. The longitudinal vortex flow may swirl around the primary flow and exhibits three-dimensional characteristics. In general, longitudinal vortices are more effective than transverse vortices from a heat transfer perspective. The imposed vortical motions provide enhanced heat transfer performance with relatively low penalty of pressure drop. This is because the pressure drop associated with wall friction is related to the derivative of the stream wise velocity (the span wise and normal velocities have little effect), but the span wise and normal velocities play a significant direct role in convective heat transfer.

Delta-Winglets are part of the third generation of fin surface enhancement methods. They are designed to generate longitudinal vortices, which are thought to be more effective in heat transfer enhancement than transverse vortices. The vortices generated are a result of the introduction or exploitation of secondary flows, rather than the manipulation or alteration of the main flow. Jacobi and Shah[6], performed a thorough review of the progress made in the application of longitudinal vortex generators. They proposed that two alternative classifications for heat transfer enhancement emerge: main-flow enhancement and secondary flow enhancement. In main-flow enhancement the gross characteristics of the flow are altered through geometric changes, pressure variations, or by other means. In secondary flow enhancement, local flow structures are deliberately introduced. In some cases, it may be difficult to distinguish between main-flow and secondary flow methods, and in some cases they may be coupled. Wavy, louvre and strip fins are examples of main flow enhancement. Delta winglets are an example of secondary flow enhancement.

Gentry and Jacobi[49] reported on heat transfer enhancement by various vortex generators mounted at the leading edge of a flat plate. They demonstrated a 50-60%

improvement in average heat transfer over the surface of the plate, using delta-wing vortex generators. They varied the angle of attack from 25 degrees to 55 degrees, with the optimum enhancement occurring at an angle of attack of 40 degrees. Their study allowed them to determine the mechanisms responsible for the enhancement. They found that streamwise vortices enhance transport by advection of free-stream (core) fluid into the boundary layer, and through this mechanism the boundary layer is effectively thinned. Vortex strength and location are important parameters in enhanced heat transfer by the vortices. The Delta-Wing geometry and angle of attack play important roles in determining how and where the vortex is started and how its position relative to the boundary layer evolves as it flows down the plate.

Figure 2.2.11 Sketch of the vortex system generated by a half-delta wing [50]

A description of the flow field formed by a delta winglet vortex generator is given by Yanagihara and Torii[50] and is schematically illustrated in Figure 2.2.11. They categorised the following identifiable vortices :

- The main vortex that is formed as a result of the flow separating in the tip of the half-delta wing and rolling up due to the lower pressure in the back side of the vortex generator

- The corner vortices that are horseshoe-like vortices formed in the corner between the front side of the wing and the fin
- The induced secondary vortex which is formed in the corner between the back side of the wing and the fin as a result of the redirectioning of the near wall flow caused by the lower pressure behind the generator.

Wang et al[3] performed a series of flow visualisation experiments to compare the flow and frictional characteristics of two types of vortex generators with that of a plain fin geometry. They used Delta wing-lets arranged in various orientations, and annular vortex generators with varying heights, located around circular tubes. The main objective of their study was to investigate the interactions of the vortices generated by the vortex generators and the horseshoe vortex normally generated at a round tube and fin junction. Although their observations were interesting, they are not particularly relevant to this discussion, and these details can be obtained from the original reference. From a qualitative point of view their observations suggested that for the same height the delta wing-let shows more intense vortical motion and flow unsteadiness than the annular vortex generators, which ultimately leads to better mixing. Their measurements also indicated that the corresponding pressure drops are lower for the delta-winglet than the annular wing-let. In general they found that the frictional penalty of these proposed vortex generators is about 10-65% higher than that of the plain fin geometry.

Punched longitudinal vortex generators forming wing-lets in staggered arrangements on the fin surface have been studied by Chen et al[8] and found to increase heat transfer by 50% and 87% with 2 or 4 staggered delta winglet pairs, respectively. Staggered wing-lets were more effective than in-line wing-lets, obtaining a 20% increase in heat transfer and 14.5% lower additional pressure loss. In the staggered arrangement, the wing-let further away from the tube was more effective for heat transfer.

Torri, Kwak and Nishino[9, 10] have proposed a novel technique that can augment heat transfer but nevertheless can reduce pressure-loss in a fin-tube heat exchanger. They performed an experimental study to evaluate heat transfer and pressure loss in a

test section comprising delta-winglet pairs arranged in a "common flow up" configuration. Here the winglets were mounted on the fin surface slightly behind the round tubes. Note that they used one row of winglets behind the first tube row only. The nozzle-like flow passages created by the winglets and the aft region of the circular tube promote acceleration to bring about a separation delay and form drag reduction of the tube, and remove the zone of poor heat transfer from the wake. The winglets were fabricated from 0.3mm thick Bakelite, which were adhered on to the fin surface. Hence, unlike punched winglets, they do not facilitate conduction and hence do not contribute an increase in the number of leading edges. Also, they do not contribute an increase in surface area, due to similar reasoning. Therefore their experiments isolate the heat transfer enhancement due to improved convection only. Unfortunately, their test core consisted only of 16 plates, and their tests were not extended to a full sized test core. They found that in the case of staggered tube banks the heat transfer was augmented by 30-10%, yet the pressure loss was reduced by 55-34% for Reynolds numbers ranging from 350 to 2100. Slightly lower improvements were achieved in the case of in-line tube banks.

A review of the current literature indicates that the so called flow-up delta winglet pair located upstream from the tube has up until now not been assessed. Normally the flow-up configuration is place downstream from the tube in order to introduce fluid into the tube wake. There are several pertinent reasons which suggest that locating the winglets upstream may prove advantageous. Therefore it behoves the initiative of this project to assess the potential of this configuration. The experimental evaluation of such a working prototype is thought to have tremendous commercial and academic interest.

2.2.2.8 Combinations of louvred surfaces with Delta-wing vortex generators

Once again reference is made to the work undertaken by Lozza and Merlo[12], having previously reported on their findings relating to the effect of the number of tube rows in section 2.2.1.2, and of wavy and louvred surfaces reported in section 2.2.2.5. Their extensive coil performance survey also covered prototypes having louvred surfaces in combination with delta-winglets. These coil prototypes had varying louvre heights as

well as extended louvre configurations, combined with 4 punched delta-winglets arranged concentrically around each tube. The combination winglet/louvred surface can be seen in the top row of Figure 2.2.10. They found unexpectedly, that there was relatively little improvement in f or j despite the winglets elevated height, 1.6mm versus a 2mm fin pitch. Upon adding a louvered section to the winglets, there was an increase in f and j but the pressure loss becomes higher than for a conventional louvered fin of comparable j. They therefore believe that the winglet design requires careful optimisation with respect to height, angle, length and location, and their current results were not sufficient for a conclusion. Or rather they concluded that enhanced fins are particularly useful for large air flows and/or reduced coil depth: with an elevated row number, their superiority over traditional fins is questionable.

Much better results have been obtained by Joarder and Jacobi[11] who experimentally evaluated a louvred radiator heat exchanger versus a vortex enhanced louvre surface. The fins were of the triangular duct type introduced by Davenport and quite common in automotive radiator applications. They placed delta-wing vortex generators at the entrance to the fins with a delta opposite the entrance to each triangular channel as shown in Figure 2.2.12 which shows a sketch of their geometric configuration.

Because of this configuration they were able to use large deltas in proportion to the louvre height, and in fact the wing to fin area ratio was 0.48%. Also the triangular channels are located between the tubes and since the vortices progression is not influenced by the tubes, the vortex strength and longevity is ensured. They reported heat transfer enhancements of up to 21% and a pressure drop penalty of less than 8%. It seems that there is a diametrically opposed viewpoint on the performance of vortex generators in combination with louvred surfaces. Apparently a delta wing placed on the fin leading edge demonstrates immense improvement in heat transfer performance, while delta-winglets located throughout the fin surface have a detrimental effect. One can surmise that any enhancement may not be generally implemented, but rather it is specific to the particular coil geometry, and therefore has to be evaluated on a case by case basis. Therefore there is scope for further investigation into the merits of combining a delta wing with the standard louvre fin surface currently investigated.

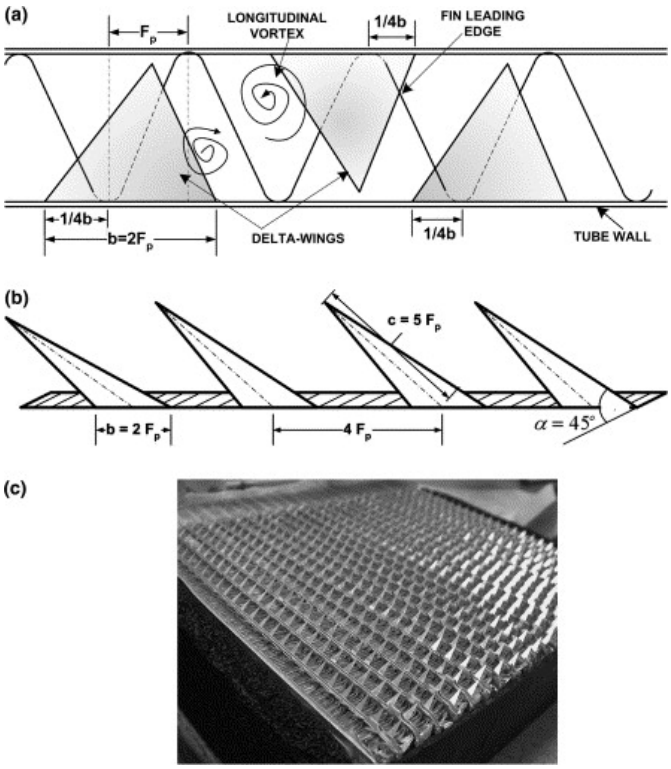

Figure 2.2.12 Vortex generator implementation (a) wing placement as shown ensures one vortex passes into each inter-fin space (b) wings are manufactured by wire EDM as strips with 10-20 wings each (c) fixing the strips to the face of the heat exchanger provides approximately 1500 delta-wing vortex generators in a staggered pattern
Figure reproduced from Joarder and Jacobi [11]

2.2.3 Tube Profiles

Round, flat and oval shaped tubes are encountered. The choice of tube shape is dependent on application rather than performance. For example round tubes are typically used for cooling and dehumidifying coils. Radiators are normally constructed with flat tubes. Round tubes are used where high internal pressures are likely to be encountered.

2.2.3.1 Elliptical or Oval shaped tubes

The air-side flow interaction with the tubes is of major importance to the pressure drop and the heat transfer area available from the tubes. It is well known that the local Nusselt number varies from a maximum at the leading edge of a tube, to a

minimum in the area of the tube wake, resulting in a low overall average. Some researchers have investigated the effect of using elliptical or oval shaped tubes on heat transfer and pressure drop. Their results were not always consistent with expectations, however. Leu et al[51] investigated numerically, the performance of both plain and louvred fins having either circular or oval shaped tubes. For one case they found that for louvred fins the heat transfer coefficients of the oval tubes were lower by about 10% than circular tubes and decreased with increasing axis ratio. However the pressure drop across the oval tubes was lower than the circular tubes by about 41% and decreased with increasing axis ratio, as one would expect. For plain fins the pressure drop of circular tubes was double that of the oval tubes. This was because the form drag contribution of the tubes was greater in proportion to the case of the louvred fin geometry. The heat transfer coefficient for circular tubes was lower at lower Re but was higher than that of oval tubes at the highest Re.

By plotting the Nu along a plane through the computational domain, they found that the highest Nu was at the front of the first tube row, and on average the Nu for circular tubes was higher at the higher Re. At low Re the average Nu for both profiles over the second tube row were the same because of the developed boundary layers. At the higher Re the Nu for the circular tubes was higher than the oval tubes at the second tube row. In general the circular tube configuration resulted in a higher average heat transfer coefficient, although the oval tube configuration had lower pressure drop. This resulted in higher goodness factors of the oval tubes than for circular tubes, especially as Re is increased.

The picture changes however, if a bank of tubes without fins is considered. Matos et al[52] performed a numerical investigation of tube banks consisting of staggered circular and oval tubes with many rows. Among the studied cases, they found that a maximum relative heat gain of 13% was achieved by the oval tubes over the circular ones for the eccentricity[16] e=0.65. In addition a pressure drop reduction of 25% was observed for the case of oval tubes compared with circular.

[16] Defined as $e=b/a$.

According to Rocha and colleagues[53], the elliptical tube geometry has a better aerodynamic configuration than the circular one, therefore one can expect less drag and better heat transfer when comparing the former to the latter. They performed a 2-D numerical analysis on one and two row tube and plate fin models, studying the effect of eccentricity. Normally a 3-D numerical model based on the Navier-Stokes and energy equations would be required to obtain heat transfer results. However, they overcame this problem by substituting experimentally obtained heat transfer coefficients from the results of others. They found that for both one and two rows, e=0.5 was the most effective. The fin efficiency associated with the elliptical tubes showed an 18% increase.

The preceding studies were conducted at steady state conditions. Obviously at certain Re vortex shedding in the tube wake would be expected to occur, perhaps to a greater degree with circular tubes rather than elliptical ones. The onset of vortex shedding can be expected to greatly enhance heat transfer throughout the applicable Re range. If the axis of an elliptic tube is rotated so that it is inclined to the approaching air stream, then one would expect a much greater degree of vortex shedding as well as an increased range of Re at which the onset of vortex shedding commences. Such a study was performed numerically by Ahmed and Badr[54]. They determined that the heat transfer performance improved with increasing Re and increasing angle of attack.

2.2.3.2 Flat Tubes

The flat tube design in combination with louvred fins is commonly used in automotive applications, and offers several advantages according to Chang and Wang[47]:

- The air flow is normal to all of the louvres;
- The wake region behind the tube does not reduce heat transfer on downstream fin regions;
- It provides a higher fin efficiency;
- The small projected area of the flat tube will result in lower profile drag than the larger diameter round tube does.

They found that the standard corrugated brazed aluminium flat tube design gives a 90% higher heat transfer coefficient for only 25% higher pressure drop compared with the round tube plain plate fin design.

2.2.3.3 Symmetrical Aerofoil Shaped Tubes

There appears to be a dearth of information pertaining to the study of heat exchangers having aerofoil shaped tubes. The closest study in this regard was conducted by Horvat *et al*[55], who numerically assessed the heat transfer and drag coefficients of tube bundles having different tube shapes. Circular, elliptic and wing shaped tubes were considered. They found that the elliptical and wing shaped tubes had considerably lower drag coefficients than the circular tubes. The wing shaped tubes had a slightly lower drag coefficient than the elliptical tubes. With regard to heat transfer they found that there was a correspondingly similar relationship amongst the tube profiles, although the difference in performance was not as great as the difference in pressure drop. This implies that although the use of wing shaped tubes has a lower heat transfer performance than circular tubes, they have a much lower pressure drop. It is feasible that a finned heat exchanger with tubes having this profile might offer similar heat capacity with lower pressure drop. A future study in this area may reveal some interesting results.

2.2.4 Tube to Tube Conduction

Some study has been done on the effect of heat transfer by tube-to-tube conduction. As a result of studies carried out by Romero-Mendez[56] can result in up to 15% decrease in heat transfer predicted, due to tube-to-tube conduction through the fin. He also points out that several authors have recognised the possibility of longitudinal tube conduction and its effects on heat exchanger performance.

2.2.5 Tube spacing

Also, with regard to tube spacing, a method was developed by Kundu[57] to determine the optimum dimension of the plate fins of a fin tube heat exchanger. He analysed both square and equilateral triangular arrays and found that under the optimum

design condition, more heat is dissipated by the fin surface for a fixed fin volume when the tubes are arranged in an equilateral triangular array.

2.2.6 Tube to Fin Contact Resistance

An experimental study has been performed by Critoph et al[58] to assess the contact resistance between fins and tubes in air-conditioning condensers. They found that under typical operating conditions, the resistance was as high as 12% of the air-side resistance. However this resistance was eliminated if an all aluminium construction along with an aluminium brazing technique was used.

2.2.7 Manufacturing Outcomes

The manufacture of heat exchangers involves very high tolerances, and any discrepancies can have repercussions on the quality of the finished product, which ultimately affects the performance in the field.

For example Lozza and Merlo[12] established while testing coils with 9 different louvre types that various manufacturing discrepancies were affecting the quality of their test coils and this was impacting on their test results. They found that the following aspects were responsible for affecting coil manufacturing quality:

- Sharpness of the louvre cutting section; if not perfect then the louvre cross section may result partially occluded, minimising the beneficial effects of the interruptions.
- Correct shape of the collar: the area contacting the tube may be reduced by a larger than necessary curvature radius.
- Thickness of the neckband collar and of the fin portion around the tube; if thinner, the fin efficiency decreases. In the worst cases, some collars may break during the tube expansion, impairing the contact between tube and fins.

There are differences in the way round tube coils and flat tube coils are manufactured. Round tube units can be fabricated inexpensively by installing the fins with a press fit on the tubes: whereas flattened tubes must be brazed or soldered to the fins in order to obtain a good thermal bond.

2.3 Alternative Heat Exchanger Designs

There are a few types of special purpose heat exchangers which have been designed for particular applications, especially in the nuclear and space industries. Although most researchers, are attempting to improve the air side heat transfer performance of the standard tube fin arrangement, there are a few projects that have been initiated in order to develop a particular configuration of a Heat Exchanger specifically designed for a particular application. Some of these are identified in this section.

2.3.1 The Pin Fin Heat Exchanger

One such heat exchanger[17] has been developed by Ko et al[59] for a project commissioned by NASA. They crafted a heat exchanger surface using flow visualisation techniques, to cater for very low Reynolds numbers as encountered by aircraft flying at high altitude. Although the heat exchanger velocities are high, the air densities at these altitudes are so low that the Reynolds numbers are in the order of 50-100, which is typically an order of magnitude lower than most available data on heat exchanger performance. Also, the available data show a rapid deterioration of the heat transfer characteristics as the Reynolds Numbers are reduced below 500-1000. Clearly, the conventional tube fin arrangement is not suitable for this Reynolds number regime, and an alternative heat exchanger surface is needed. They set out to develop and optimise a new heat transfer surface suited for this flow regime, focusing solely on the understanding and enhancement of the fluid transport mechanisms.

Their initial undertaking was a thorough examination of the heat transfer enhancement mechanisms occurring in traditional surfaces, in order to identify the flow phenomena responsible for any enhancement, and the degradation of these phenomena at low Reynolds numbers. They categorised the various traditional enhancement surfaces into three broad families: offset-strip fins, louvered fins and

[17] This heat exchanger design has formed the basis for a range of alternative heat exchanger concepts developed in this project. For this reason these findings are examined in somewhat more detail then would otherwise be the case. It is considered important to lay down the assertions postulated in this paper as the foundation upon which alternative heat exchanger designs can be developed.

wavy fins. They then surmised that the flow-related enhancement for these fins, are always associated with one of the following two mechanisms:

1. Boundary layer disruptions (renewal separation/reattachment).
2. Bulk mixing through secondary flow patterns.

They itemised the heat transfer mechanisms and reasons for degradation of performance in each of three types of commonly used fin surfaces, namely the wavy fin, the slit fin and finally the louvre fin. Their results are in line with what others have concluded, and have been discussed in this section. Having established the criteria for degradation of performance of various surfaces at low Reynolds numbers, they then went on to identify a number of desirable characteristics associated with traditional enhanced fins at higher Reynolds numbers, once again using flow visualisation. In fact they were able to identify 4 criteria that would be desirable in a heat exchanger surface as follows:

1. The surface should promote three-dimensional flow activity, even at reduced Reynolds numbers.
2. The surface should provide periodic boundary layer disruptions, even at low Reynolds numbers.
3. The surface should not promote steady, large-scale separation at low Reynolds numbers as seen in the louvered and wavy type surfaces.
4. The flow geometry should be relatively open to reduce pressure drop penalties.

Assimilating the criteria gathered up to now, these researchers were able to hypothesise a heat transfer surface that would best embody all of the desirable flow features and exclude those responsible for heat transfer degradation at low Reynolds numbers. The result is a surface referred to as a "pin fin" surface. This is schematically illustrated in Figure 2.3.1.

The geometry consists of a plain rectangular fin surface with a series of pins passing through the fins, transverse to the flow direction. They chose this configuration in order to best incorporate the characteristics discussed as they believed that it would provide the following enhancement mechanisms:

- Regions of high heat transfer coefficients in the renewed (thin) boundary layers near the stagnation region of each pin.
- Creation of transverse vorticity in the wake regions of the pins, possibly rolling into discrete vortices.
- Forced meandering of the bulk flow between the staggered array of pins, i.e. a fluidic equivalent of wavy fins in the transverse direction, without the surfaces.
- Spatially concentrating the distributed boundary layer vorticity (mean flow vorticity/shear) on the fins by rolling it into discrete vortices upstream of the pin/fin junction, hence inducing strong transport normal to the fins.
- Amplification of this localized vorticity by a ″wrapping and stretching″ of the stagnation vortex into a horseshoe vortex around the pins. This results in vortices which are now aligned in the stream wise direction on either side of the pins, also contributing to transport in the direction normal to the fins.
- Possible phase-locking in the wake regions of the pins to promote vortex shedding at low Reynolds numbers.

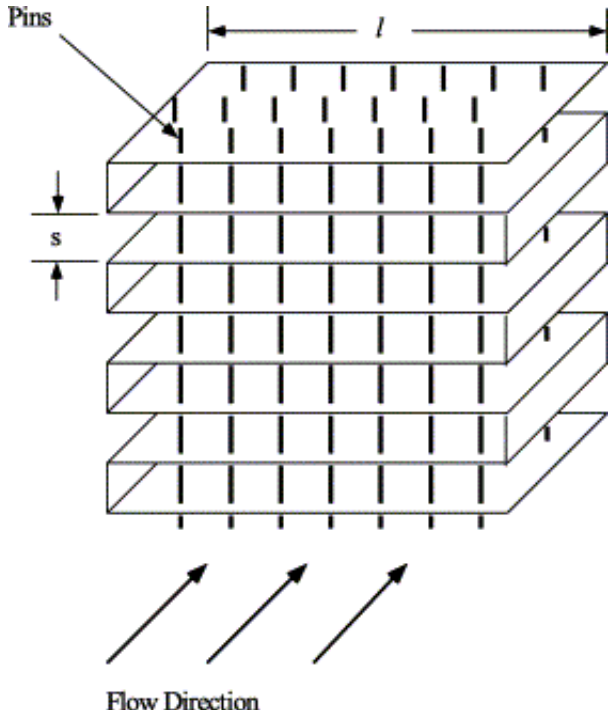

Figure 2.3.1 Sketch of the pin fin heat transfer geometry [59]

In summary, this arrangement induces strong vorticity along all three axes. Moreover, these three components are forced to interact due to their localised sources being in close proximity. Hence this geometry was designed to intrinsically force three-dimensional flow patterns and boundary layer disruptions, which are missing characteristics of most low Reynolds number flows. The researchers went on to optimise the geometry in terms of fin spacing, and pin arrangement, by observing the flow characteristics for a variety of fin and pin arrangements.

The potential for adopting this open mesh turbulence generating geometry to compact tube-fin heat exchangers has not yet been exploited. By eliminating the fins, and arranging the tubes both vertically and horizontally at widely spaced intervals into a turbulence generating mesh, the flow is not confined to narrow spaces between fins. In the absence of fins, all of the surface area is primary surface area. While it is appreciated that removal of the secondary surface area may compromise the capacity of the heat exchanger, it is noteworthy to quantify the convection enhancement due to homogeneous turbulence generation. While pressure drop measurements of mesh geometries have been extensively studied and documented by Kays and London[2], the heat transfer performance of a turbulence generating tube mesh has not been undertaken. Moreover, the experimental assessment of a tube mesh in the context of a practical heat exchanger application, so that it can be directly compared with a conventional tube fin heat exchanger is seen as having tremendous significance.

2.3.2 The Fine Wire Heat Exchanger

The principal of a fine wire heat exchanger is known from patents going back to 1927. However until recently they have been very uneconomical to produce on a commercial level. The heat exchange surface consists of a woven fabric of very fine wire as small as 100ηm, which is then attached to complementary sized small diameter tubes. At an air velocity of $0.5 m/s$ a U value of $226\, W/m^2K$ can be obtained which is around 10 times the typical value of flat plate heat exchangers to air. The heat transfer improvement is attributed to the large surface areas, and turbulence promotion by the fine wire fins.

Choi et al[60] have performed an experiment to measure the performance of several configurations of a wire woven evaporator using HCFC-22 as the working fluid. The wire diameter was $0.5mm$ and the tube diameter was $1.3mm$. They found that

compared to a similar sized tube-fin heat exchanger with $5mm$ ø tubes, the wire woven variety had 1.4-2.4 times the heat transfer capacity.

2.3.3 Patented Heat Transfer Surfaces

Wang[32, 61] has compiled a comprehensive summary of recently[18] proposed enhanced fin surface designs. Altogether he lists 51 patents that have been registered. Some of the patents are already on the market but most of them are still not available. It also appears that a reasonable quantity have been patented without having been evaluated experimentally. Wang suggests that these should be evaluated experimentally or numerically in order to gain further insight to their performance.

2.4 Parallel Plate Arrays

2.4.1 Background

As briefly touched upon in the introduction, parallel plate arrays are said to enhance heat transfer performance in comparison to that of flat plates. Figure 2.4.1 is a sketch of several examples of fins arranged to form a parallel plate array having various fin densities, reproduced from Dejong and Jacobi[7].

According to Dejong and Jacobi, there are two reasons for this enhancement. Firstly the interrupted surfaces restart the boundary layers, and since the average boundary layer thickness is smaller for short plates than it is for long plates the average heat transfer coefficient is higher for short plates than for a continuos surface. Secondly, above a critical Reynolds number interrupted surfaces can cause vortex shedding, and the self sustained flow oscillations associated with vortex shedding enhance heat transfer.

Dejong and Jacobi[7] observed that vortex shedding occurred first in the downstream rows of the array, but then moved upstream as the Reynolds number was increased. They established that there is a direct link between vortex shedding and heat transfer behaviour throughout the array. From localised heat transfer measurements using the

[18] Covering the period 1981-1999

Naphthalene sublimation technique, they were able to estimate the relative contributions to heat transfer coefficient enhancement over an equivalent continuous fin from both boundary layer restarting and vortex shedding. They found that at a Re=850 boundary layer restarting accounted for approximately 40% increase over the continuous fin result, and vortex shedding accounts for roughly another 40%. In other words, in this regime', vortex shedding and boundary layer restarting are both important mechanisms for heat transfer.

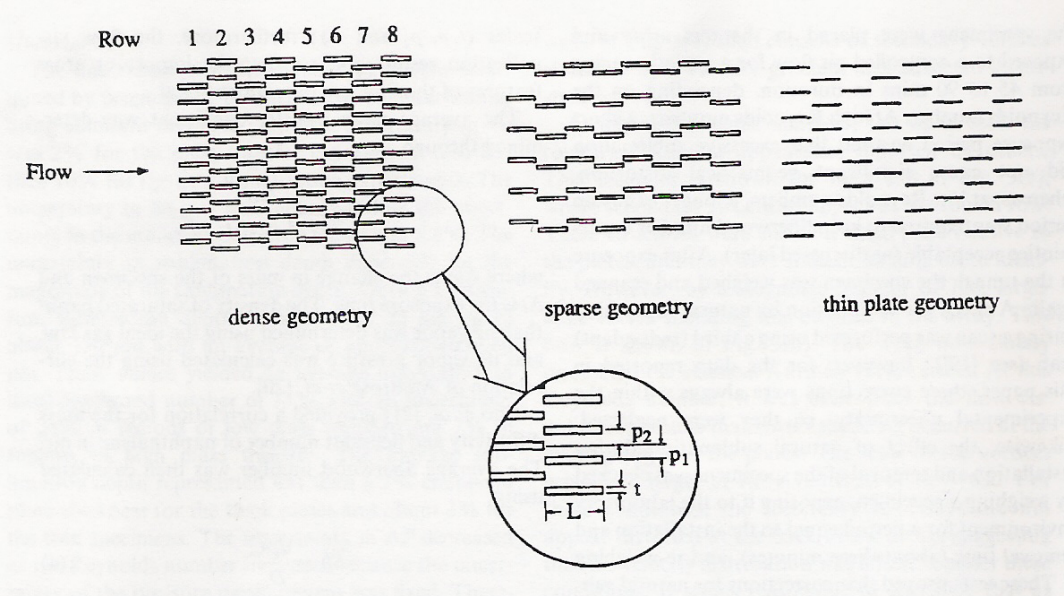

Figure 2.4.1 Sketch showing three examples of parallel plate arrays with varying geometric characteristics[7]

While they never observed shedding from the leading edge of the first row in the array, they clearly identified shedding from the second and subsequent rows. They explain the mechanism for vortex shedding as follows:

> When an upstream plate produces transverse velocity fluctuations flow at a downstream plate may separate at alternate corners of its leading edge, and this coupling causes vortex shedding at the leading edge of the plate. The first row cannot be subjected to such oscillations since there are no upstream plates to cause the oscillations.

They also observed a classical von Kármán vortex street in the wake of the array at a Reynolds number of 720.

Currently the only heat exchangers which incorporate parallel plate arrays are the offset strip fin and the slit fin geometries. The offset strip fin is normally used in a plate fin heat exchanger rather than a tube fin heat exchanger, and hence not relevant to this project. Also, since in the slit fin geometry the "plates" are punched from the fins, they are relatively thin. It is understood that the level of transverse vortices generated by the plates are a function of their thickness, and hence the vortex shedding effectiveness in this arrangement is questionable. Moreover, because of the typical fin arrangement there is bound to be suppression of any generated turbulence due to the narrow flow channels. An alternative and unique arrangement is to insert widely spaced struts in between the tubes which interconnect with the tubes to form a tube and strut mesh combination. The parallel plate arrays so formed have the potential to generate transverse vortices. In addition the numerous leading edges would facilitate boundary layer renewal. Of course, the heat transfer performance, as well as the air pressure drop is attributable to the strut spacing and thickness. Thus it is essential to develop an understanding of the highly complex fluid flow characteristics occurring in such an arrangement. The assessment of working heat exchangers having various strut thickness and spacing is seen to have enormous benefits, and the possibility of developing a sturdy, low pressure drop heat exchanger exists.

2.4.2 Parallel plate arrays combined with Delta-Wing vortex generators

There is no doubt that transverse vortices generated by parallel plate arrays enhance localised heat transfer coefficients with correspondingly lower pressure drop penalties. However the level of turbulence may not be sufficient to compensate for the reduction in surface area. This suggests combining several vortex generating methods into a single design. Smotrys et al[62] undertook a study to investigate wether incorporating vortex generators at the front of a parallel plate array would show improvement over a plain array. They used triangular shaped vortex generators to generate stream wise vortices. They found that at lower Reynolds numbers, where no transverse vortex shedding occurs, there is a heat transfer enhancement due to the stream wise vortices generated by the vortex generators. At a medium Reynolds number where the span wise vortices may be expected to start shedding, it seems interference from the stream wise vortices actually caused a reduction in heat transfer. The breakdown of span wise

vortices into chaotic unsteady flow at sufficiently high Reynolds numbers limits further heat transfer enhancement by regular vortex shedding. At higher Reynolds numbers the stream wise vortices appear to achieve dominance over the spanwise vortices, and heat transfer enhancement over a plain array is realised again.

2.5 Numerical modelling techniques

There is no commonly accepted approach to modelling the performance of tube-fin heat exchangers and choosing the appropriate models and boundary conditions is a challenging problem. Here follows a short summary of modelling techniques and boundary condition selections used by others pertaining to tube fin heat exchangers.

2.5.1 Tube Bundles

Hassan and Barsamian[63] used the LES turbulence model to simulate the flow over tube bundles, due to the flow structure in the tube wake being highly three-dimensional. They made the top and bottom of the computational domain extend over 4 rows and since these boundaries were fairly remote, they were specified as wall boundary conditions. Similarly the sides of their model were specified as wall boundary conditions.

2.5.2 Annular Fins

Mon and Gross[64] performed a study on a tube-fin heat exchanger having annular fins. They used the Renormalisation Group Theory (RNG) k-ε model, and symmetry boundary conditions for both top and bottom, as well as the sides of their computational domain.

2.5.3 Parallel Plate Arrays

A numerical simulation of flow and heat transfer through parallel plate arrays was performed by Zhang et al[65]. They performed simultaneous time-dependant and steady state calculations under otherwise identical conditions. They sought to show a difference and hence emphasise the importance of unsteady flow phenomena, as well as the importance of including three-dimensionality in the model. Interestingly they used a single plate which was bounded on all sides by periodic boundaries in their computational domain. Although the streamwise boundaries should be periodic,

(assuming a suitable description of the periodic pressure drop), it is felt that since the array was geometrically isotropic, it may have been more suitable to select symmetry boundary conditions for the sides of the computational domain. They found that in the unsteady laminar flow regime, steady flow calculations cannot represent the enhanced large scale mixing provided by coherent vortices as they traverse the fin surface.

2.5.4 Louvre Fin Geometry

Leu and Liu[51] performed a laminar, steady state simulation on a louvre fin geometry. They decided that the top and bottom boundaries should be symmetrical while the sides should be periodic. Perrotin and Clodic[66] performed both a steady laminar simulation as well as an unsteady laminar simulation having a louvre fin geometry with flat tubes, and therefore their model is particularly relevant to the current study. However, they chose symmetrical top and bottom boundary conditions while only the sides were periodic.

2.5.5 Vortex Generators

Leu *et al*[67] performed both numerical and experimental analyses of heat transfer performance and flow in plate-fin heat exchangers with block shaped vortex generators mounted in the tube wakes, using a k-ε turbulence model. They specified the top and bottom fluid boundary surfaces as well as the sides as periodic boundary conditions.

2.5.6 RANS Modelling Comparisons

Moshfegh and Nyiredy[68] trialed a range of the typical RANS models on a computational domain for a pin-fin heat sink. In addition they also varied the wall treatment to include a standard wall function (SW), an enhanced wall function (EW) and the Non-equilibrium wall approach (NW). These are optional near wall treatments which are available in the commercial CFD code Fluent and are fully described in the Fluent User Guide[69]. They found that the RNG k-ε provided the best agreement with experimental heat transfer data. However, they found that the comparison of pressure drop was not in good agreement. Furthermore, they found that the NW wall approach performed poorly, and the SW or EW wall treatment provided good agreement with the experimental heat transfer data.

2.6 Summary

It has been established that the study of homogeneous turbulence in a fin tube heat exchanger has not been investigated. This stems from the fact that homogeneous turbulence is 3-dimensional and therefore does not occur in conventional tube fin heat exchangers. The study of a grid mesh constructed of tubes which can generate homogeneous turbulence may convey useful knowledge with respect to heat transfer in a heat exchanger application.

It is evident that the scale of vortex generators and their proximity to the leading edge determine their effectiveness in heat transfer enhancement. The velocity gradients and hence shear stresses approach infinity on the leading edge. This may have the consequence of adversely affecting any imposed secondary flows such as vortex generation over a leading edge or series of leading edges, if the scale of the secondary flow is similar to that of the boundary layer thickness. The high velocity gradients and shear stresses occurring in the developing boundary layer may cause rapid dissipation of any imposed flow structure hence offsetting its designed purpose. Conversely, if the scale of the imposed flow is considerably larger than that of the developing boundary layers, then the higher vorticity levels of the imposed flow may not be as rapidly dissipated. This is especially the case if the source of the imposed flow is located some distance from the edge of the developing boundary layers where the shear stresses fall of rapidly. Therefore the effect of various vortex generating geometries such as delta-winglets or a delta wing has to be assessed on a case by case basis. Yun and Lee[70] believe that the use of interrupted surfaces has higher potential for the enhancement of heat transfer than for example scaling down the geometry, or increasing turbulence[19]. They say that for this reason, it is one of the most widely used techniques.

Transverse vortices may naturally be shed in a passive manner from a parallel plate array, while longitudinal vortices are generated typically by a vortex generator such as a delta winglet punched into the fin surface. It is reasonable to assume that a combination of these two types of vortices may have advantages over either separate

[19] Scaling down of the geometry has the effect of increasing surface area in proportion to the respective fluid volumes, but has limited practical application. Increasing turbulence may improve heat transfer, but this is also normally accompanied by a proportionally greater increase in pressure drop.

mechanism acting independently. Conversely the two entirely differing vortex structures may interfere with each other to such an extent that neither mechanism is effective, and an actual decrease in performance results. Hence the combination of different vortex generators, or possibly a vortex generator combined with an enhanced fin surface requires caution and generalisations as to the performance can not be assumed.

Irrespective of the type and nature of the turbulence generated, the full effectiveness in enhancing heat transfer can not be realised if the plate or fin spacing is too narrow. A compromise has to occur between increasing heat transfer surface area, and increasing the turbulence and three dimensional vorticity. Therefore it is essential to establish experimentally the effect of plate spacing, and plate thickness on heat transfer performance.

While enhanced surface fins demonstrate significant heat transfer improvement over plain fins, the increase in pressure losses offset these benefits by a greater amount. The heat transfer improvement is due to the local increase in velocity gradients. However, flow obstructions which may cause flow separation create an increase in pressure drop without the benefit of improving the heat transfer. The use of delta-wing vortex generators appears encouraging, although there have been diverse heat transfer enhancements reported for various types of heat exchanger geometry. There is scope for assessing other delta-winglet configurations such as a flow-up orientation located upstream from the tubes.

The performance of commercial coils can be quite sensitive to the manufacturing process. For example Lozza[12] found that testing of apparently identical coils showed significant differences in performance. They explained this to be as a result of machining and manufacturing discrepancies. The significance of this is that the performance assessment of coils is complicated by varying degrees of machining and manufacturing quality that suggests a statistical analysis in order to account for these discrepancies.

Chapter 3

Experimental Procedure

3.1 Introduction

Essentially, the experimental element of this study involved two components. On the one hand working prototypes of some of the coil designs were fabricated and experimentally assessed, and compared with the performance of commercial radiator cores. On the other hand, in some cases flow visualisation studies of scaled up perspex replicas of the prototype coils were conducted. The latter was performed in order to assist the understanding of the flow character in some of the more unconventional coil designs. These techniques were performed in order to compliment one another, rather than as a substitution of one or the other. The experimental facilities used to gather the test data or perform visualisations are described in detail. The commonly used nomenclature and equations for rating coil performance are introduced. Any subsequent deviation from the general experimental procedure shall be described in the relevant Chapter.

3.2 Coil Performance Evaluation

A series of heat exchanger prototypes were fabricated during the course of this project, each based on a specific design philosophy. The performance of each of these unique prototypes was evaluated on a purpose built coil testing facility. The apparatus and the testing technique are recited in this section.

3.2.1 Coil Testing Facility

A thermal environmental wind tunnel was used to measure the performance of the various coil prototype configurations as well as the standard louvre surface coils. The thermal environmental wind tunnel located at the University of Adelaide's Thebarton

campus, is unique in that it is a closed loop cycle. The majority of coil test facilities are open loop systems, upon which the ARI Standard 410-81[71] is based. A closed loop system is far superior to an open loop system, since precise control of the inlet conditions can be maintained. With open loop systems there can be no control over the incoming air conditions, these being subject to the environmental variations occurring within that particular laboratory throughout the day. Since the performance tests are of a lengthy duration, a wide range of inlet conditions can be expected to occur. Hence the dynamic performance characteristics of the test coil may introduce additional variables that may be considered to affect the measurements compared over various time periods.

With this closed loop system a range of temperatures and humidity's can be selected representing atmospheric conditions appropriate to most parts of the world. The control system can maintain these pre-selected conditions at entry to the coil within a fine tolerance, typically 0.1 of a degree and 2% RH. Thus the air properties and flow rate, in addition to the chilled water[1] temperatures and flow rates can be closely controlled. Since these parameters can be maintained at a constant value for any length of time, the requirement for gathering data at steady state conditions can be easily achieved. A sketch illustrating the layout of the system can be seen in Figure 3.2.1.

[1] There is also a separate Direct Expansion (DX) circuit for testing coils using refrigerant, but this was not used for the current study.

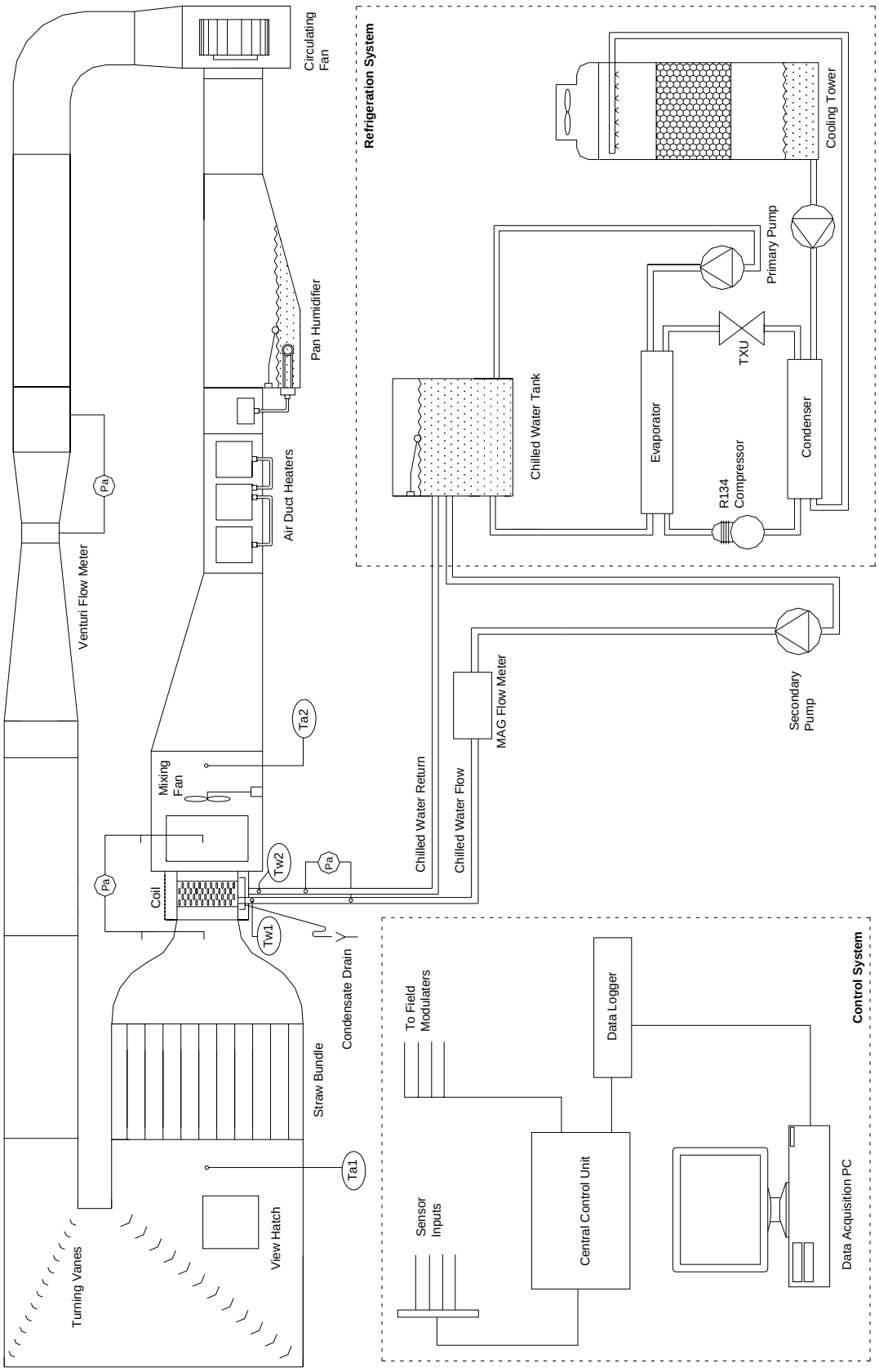

Figure 3.2.1 Sketch of the controlled Thermal Environment test rig at Adelaide University

3.2.1.1 The Air Circuit

The conditioned air is circulated through an insulated ducting system with appropriate settling sections and contractions in order to smooth and homogenise the air flow before entering the test coil. The air circuit consists of the following main components:

Variable Speed Fan: A single inlet centrifugal fan with an ABB variable speed drive circulates the air through the system. The direct digital control (DDC) variable speed drive is capable of varying the on coil air flow rates from $0.4m^3/s$ to $1.6m^3/s$ at a speed of 3250 rpm. This air flow rate provided a maximum on coil air face velocity of over 8 m/s for the current test coils which measure 760mm wide by 260mm high.

Venturi: The venturi section has been designed according to ISO standards, which incorporate British Standards, and enables accurate measurement of air flow through the apparatus during tests. A digital pressure transducer recording the venturi pressure drop is used to directly control the speed of the variable speed fan.

Settling section: From the venturi the duct transforms from a round section to a larger square section where turning vanes ease the airflow through two 90° bends. A large settling chamber reduces the air velocity and provides a large thermal reservoir to prevent temperature fluctuations. The air then passes through a honeycomb screen and a packed bank of drinking straws removes any axial swirl from the air stream entering the test coil and establishes a consistent length scale for the turbulence in the flow. After the settling chamber the air passes through two contraction sections which further homogenise the flow and reduces the cross section of the duct to match that of the test coil.

Test Coil Section: The test coil section is removable to facilitate the installation of coils to be tested. This section can accommodate coils with various aspect ratios up to a maximum size of 760x760mm. However for this study the size of each test coil was maintained at 260mm high and 760mm wide. Apart from minor variations in the depth of each coil, the test coils all had 4 rows and a corresponding depth of approximately 60mm. The test coil was encased in an insulated casket consisting of 50mm thick polystyrene sheeting. The gaps were taped over with silver duct tape to

thoroughly eliminate any potential heat leakage paths and ensure a good energy balance between the air and water circuits. The downstream section of the test coil is immediately followed by a free turning windmill to ensure thorough mixing of the air leaving the test coil before the off coil temperature and humidity measuring station. The coil test section also has the facility for removing any condensate generated on the coil surfaces while maintaining a balanced pressure in the test section so that no air leaks into or out of the system.

Reheater section: Downstream from the temperature and humidity sensor, the duct slopes downwards before entering the re-heaters. The purpose of the slope is to provide sufficient displacement of the electric duct heaters from the temperature sensor so that the possibility of radiation affecting the off coil temperature is eliminated. The re-heater section consists of electric heating elements that are automatically controlled by the DDC control system to precisely maintain the on coil air temperature to the air temperature set point. It is important to note that the air temperature sensor for the duct heater controller is located just after the variable speed fan upstream of the venturi meter, and not from the on coil temperature measurement. This is to ensure rapid response to variations in the off coil temperature. The huge volume of air in the settling section would introduce too much lag in response to any temperature variation to provide adequate control of the air heaters.

The Pan Humidifier: Directly after the duct heating section, the pan humidifier consists of a shallow sump below the level of the duct containing water which contains an electric water heating element. The controller for the heater element generates saturated steam which humidifies the air according to the desired humidity set point. Water makeup is provided through a ball valve which maintains the level of water in the sump or pan.

3.2.1.2 The Water Circuit

The water circuit consists of two combined circuits. The primary chilled water circuit circulates chilled water generated by the refrigeration circuit to an insulated storage vessel raised above the heat and mass flow test rig. A primary pump circulates the water from the tank through the refrigeration circuit and back until the desired chilled

water set point temperature has been reached. In the secondary circuit, a secondary pump circulates chilled water from the storage tank through a delivery gate valve and then to the test coil. From the test coil the chilled water then returns to the storage tank. Make up water is supplied to the tank after passing through two fibre media filters to eliminate the possibility of fouling the test coils with algae or dirt. The chilled water flow rate can be controlled by throttling the flow using the delivery gate valve. The flow rate could be delivered to the test coil up to a maximum of $140 l/m$.

3.2.1.3 The Refrigeration Circuit

The refrigeration circuit consists of the following main components:

Compressor: A semi hermetic reciprocating compressor driven by a variable speed drive motor is used. The compressor uses R134a refrigerant, and has a cooling capacity of approximately $21 kW$.

Evaporator: This is a shell and tube evaporator which is controlled with an automatic variable volume expansion device.

Condenser: This is a shell and tube condenser.

Cooling Tower: A water cooled forced draught cooling tower facilitates the rejection of heat to atmosphere.

3.2.1.4 Instrumentation

The entire system is controlled with a DDC control system with a front end computer running instantaneous display software so that timelines of the various measured variables could be monitored over lengthy time intervals.

Air Temperature: This was measured using VIASALA combined temperature and humidity sensors. The on coil measurement was located in the settling chamber just upstream of the straw bundle. The off coil measurement was located slightly

downstream from the free turning windmill, to ensure that effective mixing of the air took place. The temperature sensors have an accuracy of 0.1°C.

Water Temperature: The chilled water temperature was measured using two PT100 platinum resistance thermometers having an accuracy of 0.1°C, located in 90° brass elbows directly adjacent to the coil inlet and outlet manifolds as shown in Figure 3.2.2. The sensors were mounted in a brass resealable coupling which made it convenient to be able to remove and replace the sensors during installation of the test coil. By mounting the sensors virtually on the bend of the elbow, it ensured that any temperature stratification was minimised due to the turbulence in the elbow[2].

Figure 3.2.2 Photograph showing the location of the PT100 water temperature thermometers

[2] In previous tests where the sensors were located directly in the manifolds, temperature stratification of the water led to temperature measurements which did not provide values which resulted in an acceptable energy balance with the air flow. With the current arrangement, an energy balance of within 5% was achieved at most flow rates.

Air Flow: This is measured by the venturi which was manufactured in accordance with British Standard Code BS 1042: 1967. At the neck of the Venturi, as well as a location in the circular duct upstream of the Venturi, pressure tappings are distributed around the circumference and connected to a piezometer ring. The differential pressure is sensed by a capacitance-type differential pressure transducer with an accuracy of ±0.5%.

Coil Air Pressure Drop: The pressure drop across the depth of the coil was measured by an upstream and downstream pitot tube. Since there was a difference in duct size at these locations, the pitot tubes were connected so that they recorded Total pressure, in order to account for any static pressure recovery resulting from the change in duct size. The pressure differential was recorded by a capacitance-type differential pressure transducer with an accuracy of ±0.5%.

Coil Tube water pressure drop: This was recorded using a capacitance-type differential pressure transducer. The probe locations were some distance upstream and downstream from the coil. This meant that the tube pressure drop included the contribution from the manifolds as well as some length of flexible tubing. Due to the permanence of the sensor locations this error could not be avoided. However as most of the test coils had the same number of tubes and the same manifold configuration this additional pressure drop would apply equally to each test coil. In any event, the tube pressure drop was not of significant interest in our current investigation of fin surface performance, and was only recorded as a matter of fact.

Water flow rate: This was measured using an ABB Magmaster Flowmeter for measuring the water velocity through a calibrated pipe section. The ABB Magmaster is fitted with a CalMaster diagnostic monitoring tool and has an accuracy of approximately 1%.

Calibration: The instrumentation was calibrated and then checked periodically. Through experience it was observed that between test coils, the capacitance-type differential pressure transducers were prone to drift and therefore these were checked before each coil was tested.

3.2.1.5 Coil testing methodology

The coil testing procedure specified by ASHRAE Standard 33-78 and ARI Standard 410-81 involve a very comprehensive evaluation of each coil. Since these standards require that any measurements are recorded not sooner than 30 minutes after thermal equilibrium has been attained, the test procedure can be very lengthy depending on the number of test points required. The time period specified by these standards apply to an open cycle system which is highly influenced by ambient conditions and is therefore necessary in order to eliminate any variables in measurement arising from the transient response of each test coil. The coils assessed in this study were tested in a closed cycle system which was independent of any variation in ambient conditions. Under most operating conditions, it was unproblematic to establish and maintain thermal equilibrium for an indefinite period. In most cases once thermal equilibrium was attained, there was no variation in the off coil conditions so that it was immaterial how long after steady state condition was reached before recording any measurements. Nevertheless, in maintaining strict accordance with the test procedures, a time period of 30 minutes was allowed to elapse before each set of readings was recorded. The only time when maintaining steady state conditions for a long period of time became problematic, occurred when testing a coil which was operating at a capacity equal to or perhaps greater than the cooling capacity of the refrigeration system. The thermal reservoir of chilled water is limited by the storage capacity of the chilled water storage tank, which is only 0.6m^3. As the volume of stored chilled water was expended, the chilled water supply temperature to the coil, and hence the chilled water leaving temperature would begin to drift upwards. Since the change in water temperature across the coil would remain constant, the calculation of capacity would be unaffected by the temperature drift. However the calculation of UA and hence U would be affected by the discrepancy in $LMTD$ arising from the drift in supply temperature. In order to eliminate this problem, the supply temperature set point was set at 11.5°C rather than a typical chilled water temperature used in an air conditioning coil of say 6°C. This effectively increases the capacity of the compressor, and reduces the capacity of the coil being tested since the $LMTD$ across the coil is less for a fixed inlet air temperature. An additional measure adopted to increase the refrigeration capacity was to test a high capacity coil when the outdoor ambient temperature was low so as to reduce the refrigerant condensing temperature. This

subtle measure delivered some additional refrigeration capacity from the system. In general even the high performance commercial coil having a louvred surface at 11 fpi was able to be tested at maximum capacity without any drift in temperature during the testing period.

3.2.1.6 Standard Heat Transfer analysis

The ASHRAE Standard 33-78 and ARI Standard 410-81 allow for a broad range of test temperature settings and fluid flow rates. Normally one is interested in the air side performance of a particular fin surface geometry since the fin surface configuration is tantamount to the overall coil performance. As such, the water flow through the tubes is appropriately selected and then held constant for all test conditions. It is the air velocity that is varied so that the fin performance is evaluated under varying air flow conditions. However, in the case of unconventional heat exchangers, it is more appropriate to compare the overall heat transfer coefficient U values since there may be a large variation in heat transfer surface area. Also, it was considered appropriate to assess the performance of some of these unconventional coils at various tube flow rates in order to gain understanding of the coils overall performance. This was especially the case for example when testing the Tube Mesh coil which had two supply manifolds and two return manifolds.

A generalised procedure is outlined here, but a prototype specific procedure may be specified in the relevant chapters.

- The chilled water temperature set point was set at 11.5°C, and the air on coil dry bulb set point was 40°C. This gave a practical temperature difference of working fluids through the test coil.
- The air on coil face velocity was set at 2.9m/s, 4.8m/s and 6.3m/s.
- For each air velocity, the water flow rate was set at 40, 60, 80, 100 and 120 l/min. This corresponded to tube velocities of $0.85 m/s$ to $2.5 m/s$
- Once steady state condition had been reached and maintained for 30 minutes, the measured variables were recorded
- The Data Logging computer was loaded with software which facilitated a display of an instantaneous readout of the measured variables. A time interval

of 60s was specified over which the logged variables were averaged at the time of measurement.

- The measurements were recorded on a data collection template along with any comments or significant observations during the test.
- The recorded data was then entered into a Microsoft Excel spreadsheet where it could be easily reduced and exported to other software packages.

Initially, the earlier prototypes were compared on the basis of heat transfer capacity, U value and the measured pressure drop. The following equations were used to determine the capacity and overall heat transfer coefficients.

The capacity of the coil based on the air temperature difference is

$$\dot{Q}_a = \dot{m}_a c_{pa} \Delta T_a \tag{1.1}$$

The corresponding capacity based on the water temperature difference is

$$\dot{Q}_w = \dot{m}_w c_w \Delta T_w \tag{1.2}$$

These two values typically were within 5% of each other, and the average was used to determine the overall heat transfer coefficient or U value, hence

$$\dot{Q}_{ave} = \frac{\dot{Q}_a + \dot{Q}_w}{2} \tag{1.3}$$

The average heat transfer capacity is equated to the basic heat transfer equation

$$\dot{Q}_{ave} = UA_o \cdot F \cdot LMTD \tag{1.4}$$

The *LMTD* is evaluated from

$$LMTD = \Delta t_m = \frac{(t_{ai} - t_{wo}) - (t_{ao} - t_{wi})}{\ln\left[\frac{t_{ai} - t_{wo}}{t_{ao} - t_{wi}}\right]} \tag{1.5}$$

The F factor is the appropriate correction factor applied to account for the deviation from a pure counter-flow arrangement. The tube-fin coils tested in this study were considered to be in the category of cross flow with *both fluids unmixed*. It is understood that in the case of heat exchangers having a complex geometry such as the Tube Mesh or Tube Strut heat exchangers which have multiple leading edges on the air side, and hence diverging flow paths, an F factor may not be meaningful. However since the flow in these coils is still essentially 2-dimensional, using the same category of F factors is considered appropriate. These were obtained from Figure C.4b on page 931 of Mills[36]. It was found that at the range of fluid operating temperatures tested, the F factors were between 0.96 and 0.98, and hence would have negligible effect on the results anyway.

Rearranging equation (1.4) we get

$$UA_o = \frac{\dot{Q}_{Ave}}{F \cdot LMTD} \tag{1.6}$$

And finally the overall U value is

$$U = \frac{\dot{Q}_{ave}}{F \cdot LMTD \cdot A_o} \tag{1.7}$$

3.2.1.7 Error analysis

The uncertainty in the results is due to an accumulated error caused by the inaccuracy of the instrumentation, and the experimental error owing to the temperament of the

experimental setup. This error is attributable for the discrepancy in the heat transfer energy balance between the two fluids. Heat loss in the equipment due to air leakages, water temperature sensor locations and insulation shortfalls are responsible. In 95% of measurement results the energy balance is less than 5% which is an acceptable limit for this type of experiment according to ARI Standard 410[71] and other active researchers in this area for example Wang[72]. However by taking an average of the air and water heat transfer, the experimental error is minimised if not negated altogether.

An uncertainty analysis due to the measurement inaccuracy was conducted according to the Kline and McClintock method[73]. The test data gathered for the louvre fin coil with 11 *fpi* was used to estimate the uncertainty. The cases of the lowest fluid flow rates and contrastingly the maximum fluid flow rates were selected.

An estimate of the uncertainty in a calculated result on the basis of uncertainties in the primary measurements is given by,

$$R = R(x_1, x_2, x_3, ..., x_n) \tag{1.8}$$

Let e_r be the uncertainty in the result and $e_1, e_2, ..., e_n$ be the uncertainties in the independent variables. The uncertainty in the result is given by,

$$e_R = [(\frac{\partial R}{\partial x_1} e_1)^2 + (\frac{\partial R}{\partial x_2} e_2)^2 + ... + (\frac{\partial R}{\partial x_n} e_n)^2]^{\frac{1}{2}} \tag{1.9}$$

These two experimental set points have been highlighted in the experimental data tables located in Appendix IV. The basis of the examination involves estimating the uncertainty of the measured heat transfer capacity found from Equation(1.1) and Equation(1.2). Since all the other parameters such as U and UA are found from these equations, they can also be considered to have the same degree of measured uncertainty. The details of the uncertainty analysis calculations are described in detail in Appendix V, and a summary of the results is tabulated in Table 3.1.

Table 3.1 Summary of results from an uncertainty analysis for the case of the Louvre fin coil having 11fpi, at minimum and maximum flow rates. The calculations can be found in Appendix V

Flow Settings	$\dot{Q}_a$	$\dot{Q}_w$	% Energy Balance	$e_{\dot{Q}_a}$	$e_{\dot{Q}_w}$	% $e_{\dot{Q}_a}$	% $e_{\dot{Q}_w}$
Air vel=2.9m/s Water Flow=40L/min	11486.01	11097.92	3.37	111.20	415.65	0.97	3.75
Air vel=6.3m/s Water Flow=120L/min	21607.34	21288.67	1.47	228.02	2450.44	1.06	11.5

For this particular sample of results it is apparent that the energy balance in the case of the minimum fluid flow rates is greater than for the maximum fluid flow rates, but both results are well below the acceptable value of 5%. The uncertainty in the air heat transfer is approximately 1% in each case. At minimum fluid flow rates the water heat transfer uncertainty is only 3.75% but at the maximum fluid flow rates it is as high as 11.5%. Clearly at high water flow rates the ΔT is small and hence the percentage error is high. Since the calculated heat transfer is an average of the air and water heat transfer values the maximum calculated error occurs when either the two maximum values or the two minimum values occur simultaneously. In this case the error for the case of the maximum fluid flow rates, which clearly has the greatest measurement error of 11.5%, was found to be 6.24% when averaged. Note that this is the maximum error calculated for the extreme case. In general the energy balance was less than 5% in the majority of cases.

3.2.1.8 Determination of Colburn *j* Factor

Conventional coil testing usually rates the non dimensional air-side heat transfer coefficient or Colburn *j* factor. Therefore it is important to present the data so that it can be compared with fin designs suggested and measured by others. To be consistent with the procedure conducted by other researchers, performance plots of the Colburn *j* factor, and the fanning friction factor *f*, need to be presented as a function of air Reynolds number. The following Data Reduction method has been adopted from Wang *et al*[72].

The air-side thermal resistance is typically obtained from the overall thermal resistance equation

$$\frac{1}{UA_o} = \frac{1}{\eta_o h_o A_o} + \frac{1}{h_i A_i} + \frac{\delta_w}{k_w A_w} \tag{1.10}$$

Some researchers attempt to take into account the contact resistance between the tube and the fin, and therefore add an additional resistance term to equation (1.10). Wang *et al*[72] suggests that this can be the source of uncertainty, and logically should be included in the air-side thermal resistance. Since, in the case of the entire test coils assessed in this study, the coil fins were baked onto the tubes coated with tin solder, the contact resistance was considered minimal and hence the contact resistance was included as part of the air-side thermal resistance.

The air-side thermal resistance $1/\eta_o h_o$ is obtained by subtracting the tube-side resistance and wall resistance from the overall resistance, ie.

$$\eta_o h_o = \left(\frac{1}{U} - \frac{\delta_w A_o}{k_w A_w} - \frac{A_o}{h_i A_i} \right)^{-1} \tag{1.11}$$

Wang *et al*[72] recommends that for precise evaluation of $1/\eta_o h_o$, the water-side and wall thermal resistance be small in comparison to the total thermal resistance, and the water-side heat transfer coefficient h_i should be accurately evaluated. In order to reduce the waterside thermal resistance, the water flow rate was set at the maximum possible ie 120*l/min*. For a single-phase fluid flowing in a smooth tube, h_i may be evaluated from the Gnielinski semi-emperical correlation:

$$h_i = \left(\frac{k}{D} \right)_i \frac{(\mathrm{Re}_i - 1000)\,\mathrm{Pr}(f_i/2)}{1 + 12.7\sqrt{f_i/2}\,(\mathrm{Pr}^{2/3} - 1)} \tag{1.12}$$

where

$$f_i = (1.58 \ln(\mathrm{Re}_i) - 3.28)^{-2} \tag{1.13}$$

and

$$\mathrm{Re}_i = \rho V_i D_i / \mu \tag{1.14}$$

The second term on the right hand side of Equation (1.11) accounts for the thermal resistance of the tube wall and A_w is calculated using the internal wall hydraulic diameter.

In order to calculate UA_o, the $\varepsilon - NTU$ method is used, and the appropriate relationship for an unmixed/unmixed cross flow arrangement is

$$\varepsilon = 1 - \exp\left[NTU^{0.22} \cdot \left\{ \exp(-C^* \cdot NTU^{0.78}) - 1 \right\} / C^* \right] \tag{1.15}$$

ε and C^* can be determined from the operating conditions using,

$$\varepsilon = \frac{\dot{Q}_{ave}}{\dot{Q}_{\max}} = \frac{\dot{Q}_{ave}}{(\dot{m} c_p)_{air} (T_{in,water} - T_{in,air})} \tag{1.16}$$

$$C^* = \frac{C_{\min}}{C_{\max}} = \frac{(\dot{m} c_p)_{air}}{(\dot{m} c_p)_{water}} \tag{1.17}$$

and also $NTU \equiv UA / C_{\min} = fn(\varepsilon, C^*)$. A trial and error method was used to evaluate NTU by guessing values of NTU until the guessed value produced the correct ε value, correct to two decimal places. Hence using Equation (1.11) the product $\eta_o h_o$ could be determined. However, before h_o can be evaluated it is necessary to determine the surface efficiency η_o, but before that the fin efficiency η. The surface efficiency is related to the fin surface area as follows

$$\eta_o = 1 - \frac{A_f}{A_o}(1-\eta) \tag{1.18}$$

where

$$\eta = \frac{\tanh(mr\phi)}{mr\phi} \tag{1.19}$$

$$m = \sqrt{\frac{2h_o}{k_f \delta_f}} \tag{1.20}$$

and

$$\phi = \left(\frac{R_{eq}}{r} - 1\right)\left[1 + 0.35\ln(R_{eq}/r)\right] \tag{1.21}$$

R_{eq} is a geometrical parameter which takes into account the pitch and alignment of the tubes while r is the tube radius including the fin collar thickness.

For plate fins Schimdt[74] has shown that Equation (1.19) may be applied if the following definition is used to find R_{eq} for the staggered[3] tube layout

$$\frac{R_{eq}}{r} = 1.27\frac{X_M}{r}\left[\frac{X_L}{X_M} - 0.3\right]^{1/2} \tag{1.22}$$

where XL and XM are geometric parameters defined as

$X_L = \sqrt{(P_t/2)^2 + P_l^2}$ for a staggered tube layout and

$X_M = P_t/2$

[3] There is a corresponding relationship for an inline tube layout but is not relevant to this analysis.

Wang *et al*[72] suggest that preferably the values of $\frac{R_{eq}}{r} < 3$ in order to limit error to 5%, and similarly $m(R_{eq}/r) > 2$. In order to obtain values within these limits, it was necessary to convert the flat tube outer perimeter of the coils used in this study into an equivalent circular perimeter.

It can be seen from Equation (1.20) that in order to determine m, it is necessary to know the value of h_o. Hence an iterative procedure is required in order to determine h_o and m simultaneously. By using the calculated value of h_o (after an initial guess) as a guess for the following iteration, a level of accuracy to two decimal places could be achieved within 4 or 5 iterations.

Finally the Colburn *j* factor can be found from

$$j = \frac{Nu\,\mathrm{Pr}^{-1/3}}{\mathrm{Re}_{Dc}} \tag{1.23}$$

and

$$Nu = \frac{h_o D_c}{k} \tag{1.24}$$

Note that the definition of Reynolds number in equation (1.23) is based on the tube plus collar diameter in the case of circular tubes. Since the coils in this study had flat tubes, the tube dimension across flats plus the fin thickness has been used as the equivalent length scale. This is the length scale that is most appropriate to influence the velocity field.

Substituting equation (1.24) into equation (1.23) we get

$$j = \frac{h_o\,\mathrm{Pr}^{2/3}}{c_p G_c} \tag{1.25}$$

Where G_c is the mass velocity = ρV_c

3.2.1.9 Determination of fanning friction factor *f*

In order to account for entrance and exit losses in determination of the coil friction factor, Kays and London[2] have supplied the following pressure drop equation.

$$f = \frac{A_c}{A_o}\frac{\rho_m}{\rho_1}\left[\frac{2\rho_1\Delta P}{G_c^2} - (K_c + 1 - \sigma^2) - 2\left(\frac{\rho_1}{\rho_2} - 1\right) + (1 - \sigma^2 - K_e)\frac{\rho_1}{\rho_2}\right] \qquad (1.26)$$

The term σ is a contraction ratio to account for the reduction in flow area caused by the fins and tubes. Thus it is the ratio of the minimum flow area to frontal area and depends on the fin and tube geometry. Depending on the core configuration, K_c and K_e can be found in Kays and London[2] who provide plots for various geometries, however none of these correspond to a fin tube heat exchanger. The alternative and far more logical approach is to include the effect of the entrance and exit losses in the core friction term as follows:

$$f = \frac{A_c}{A_m}\frac{\rho_m}{\rho_1}\left[\frac{2\Delta P\rho_1}{G_c^2} - (1 + \sigma^2)\left(\frac{\rho_1}{\rho_2} - 1\right)\right] \qquad (1.27)$$

3.3 Flow visualisation

As the possibility of vortex formation has been suggested and indeed aimed at in the design of the various heat exchangers tested, the flow characteristics were of interest. A flow visualisation study was undertaken in a qualitative manner in order to discover wether stream wise vortices were induced, and how they would interact with the rest of the flow field. The intention was not to quantify the intensity of any vortex formation which would require more advanced velocity measurement techniques, which are beyond the scope of this particular project. It was purely intended to perform a

visual appraisal of the flow characteristics, and hence deduce the effect on potential heat transfer improvements.

3.3.1 Low-vibration water tunnel

The water tunnel used for the flow visualisation experiments had the advantage of being mechanically decoupled from the water recirculation pumps and the weir discharge. This was achieved by installing a siphon system at the supply end of the tunnel. Thus the inlet water flow was transferred from the supply tank to the tunnel through 5 separate siphon tubes, which were mechanically isolated from the tunnel. This minimised any vibration and high velocity fluid arising from the pumps being transferred to the working section of the tunnel. Similarly, the discharge flowed into a tank which was not attached to the tunnel. It was found that the free stream turbulence in the working section was minimal up to a water velocity of $0.1m/s$. The water velocity was controlled by throttling the butterfly valves located at the discharge of the centrifugal pumps. The working cross section measured 350mm high by 175mm wide. A sketch of the water tunnel can be seen in Figure 3.3.1.

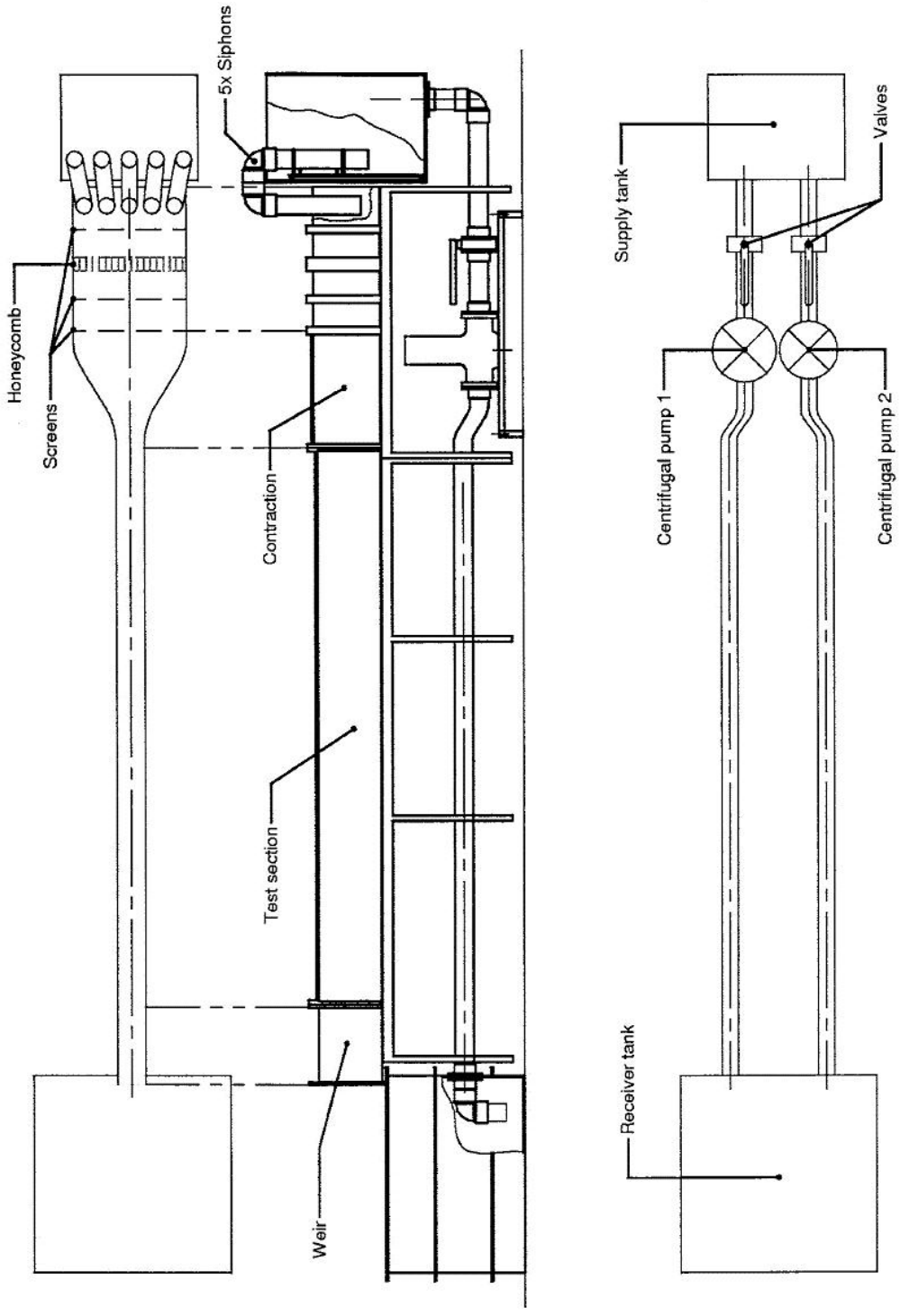

Figure 3.3.1 Sketch of the Low-vibration water tunnel at Adelaide University

3.3.1.1 Flow calibration

The various perspex models were tested at three different velocities which corresponded to the equivalent Reynolds numbers of the air velocities used in the measurement of actual coil prototype performance. A hydrogen bubble generating wire was used to generate timelines which flowed past a scaled distance at a particular flow. A scaled photograph of the timelines was taken, so that the distance between the timelines could be accurately measured. Hence knowing the frequency of timeline generation, the velocity could be accurately determined. The three velocities of interest were all measured with a water level in the working section being 287mm high. This was sufficient to cover the models comfortably. At each velocity, the height of the weir was measured, as well as the height of the nappe. Thus once these settings had been determined it was straightforward to select the appropriate velocity by adjusting the pump flow rate until the water height at the model was equal to 287mm.

3.3.1.2 Dye release technique for Parallel Plate Array models

Two different dye release techniques were used depending on the geometry of the models used. The models simulating the Parallel Plate Array heat exchangers were built at a 3 times scaled up version of the real coil. These were tested at water flow velocities of 0.07, 0.11 and $0.15 m/s$ which corresponded to 2.9, 4.8 and $6.3 m/s$ air face velocity over the working prototypes. It was found that the least obtrusive manner of releasing the dye was from within the model itself. A coaxial hole was bored down the length of three middle tubes at the front of the model. A 1.5mm hole was bored into the stagnation point on the tube diameter until it intersected with the coaxial tube. The other end of the Perspex tube where it emerged through the backing plate was plugged with a grommet and a surgical tube. Thus a gravity feed system could be used to feed dye through the surgical tube and would discharge into the water at the tube stagnation point. This is explained more clearly with diagrams in Chapter 6 dealing with Parallel Plate Arrays. Three dye colours were supplied to the model from three suspended intravenous drip tubes. Supplying the dye from a drip tube was advantageous because instead of emptying, the tube deflated, allowing the dye to be supplied at a constant pressure for reasonably long durations.

3.3.1.3 Dye release technique for Delta Wing Vortex generators

Unlike the Parallel Plate Array models in which the struts were built from 1.5mm thick sheets, the modelling of 0.076mm thick copper finstock was more challenging. It was decided to build a 6 times scaled up model of each proposal. This meant that the fins could be reasonably modelled using 0.5mm thick PVC sheeting. In addition the corresponding test velocities would be half of those used previously ie 0.04, 0.06 and $0.08 m/s$. These lower velocities considerably reduced free stream turbulence and allowed a dye release probe to be mounted upstream of the models with no vortex or other turbulence shedding. The dye release probe was mounted in a dial gauge stand which allowed a smooth vertical traverse of the tank to be made. Therefore a single dye probe could be shifted to cover and hence facilitate visualisation of the regions of interest. A photograph demonstrating how the probe was mounted can be seen in Figure 3.3.2.

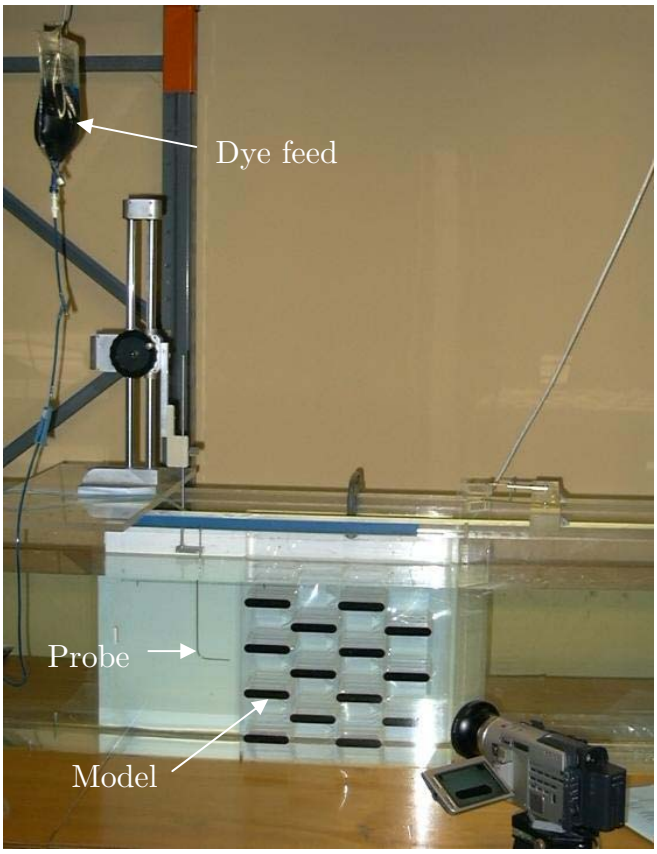

Figure 3.3.2 Photograph showing the Dial Gauge stand for mounting of the dye release probe

The model consisted of a backing plate on which the tubes were mounted in the appropriate staggered array. At this scale the resulting tube bank completely filled the width and depth of the tunnel working section. For each turbulence, or vortex generating proposal, three fins were made by cutting out diagonal shaped flaps for the tube holes, and the particular winglet shape of each vortex generator. The vortex generator was then formed by bending the various winglets through 90^{o} along one edge. Once these winglets had been bent in place, although they were still flexible, the shape of the winglet was reasonably rigid and locked into the correct orientation. The three PVC fins were then slotted down the shaft of the tubes until they were positioned approximately in the centre of the tunnel.

3.3.1.4 Controlling the velocity profile entering the model

Since the models or at least the fins of the models may not span the entire cross section of the tunnel, it was necessary to compensate for any fluid that may preferentially bypass the model and therefore compromise the desired uniform velocity profile entering the model. Figure 3.3.3 is a photograph depicting the arrangement of flow control baffles which were used to regulate this.

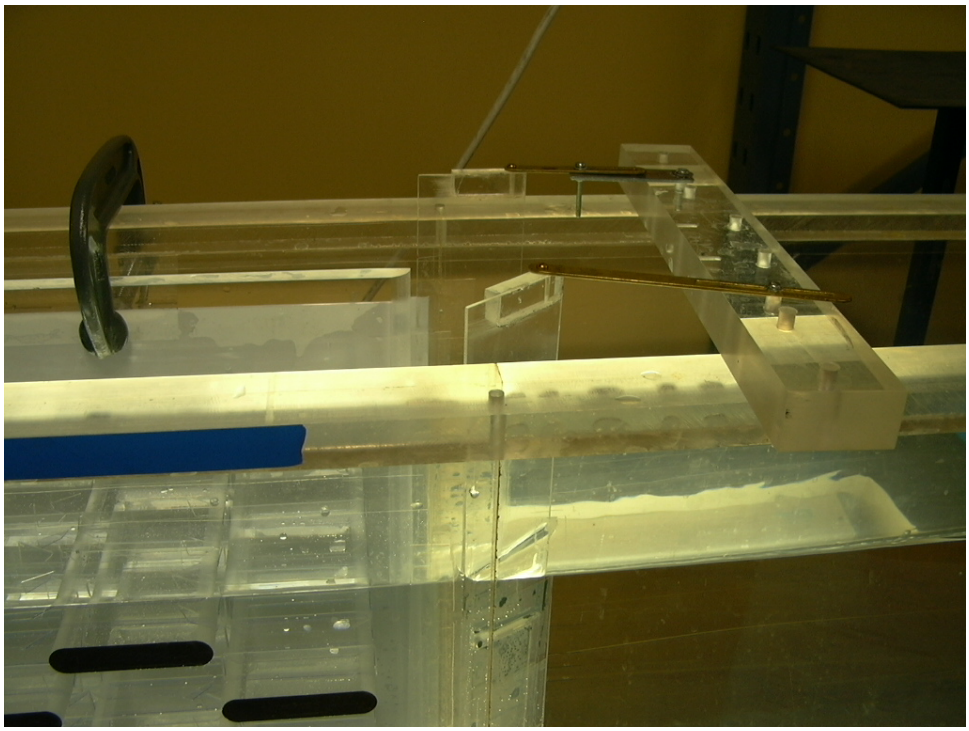

Figure 3.3.3 Photograph of the flow control dampers to promote uniform velocity entering the model

Perspex sheets were hinged to either side of the model, and if necessary to the bottom of the model. These flaps could then be used as baffles to throttle the flow around the edges of the model creating an artificial pressure drop so that a near uniform velocity profile across the entry to the model could be achieved. This was verified by monitoring any bias in direction of a dye trace entering the model. The baffles were adjusted until the dye entered the model without any bias.

3.3.1.5 Video capture technique

A Sony digital video camera with a resolution of 720x576 and a frame rate of 25 frames/second was used to capture video footage for each setting. The dye was gradually released into the centre of the model, by controlling it with the intravenous drip valve until a smooth and clearly visible stream of dye was observed. Two zoom settings were used to capture a) detail of the flow field specifically around the middle vortex generator, and b) the flow field through the entire tube array. Unfortunately in the case of the latter, the dye dispersion after the first vortex generator, combined with the wider capture angle, meant weak visibility of the overall flow field.